

T-2326

SECOND VERTICAL DERIVATIVE
ENHANCEMENT OF
DIRECT CURRENT BIPOLE-BIPOLE DATA

by

Brandon R. Brygider

ProQuest Number: 11016643

All rights reserved

INFORMATION TO ALL USERS

The quality of this reproduction is dependent upon the quality of the copy submitted.

In the unlikely event that the author did not send a complete manuscript and there are missing pages, these will be noted. Also, if material had to be removed, a note will indicate the deletion.



ProQuest 11016643

Published by ProQuest LLC (2019). Copyright of the Dissertation is held by the Author.

All rights reserved.

This work is protected against unauthorized copying under Title 17, United States Code
Microform Edition © ProQuest LLC.

ProQuest LLC.
789 East Eisenhower Parkway
P.O. Box 1346
Ann Arbor, MI 48106 – 1346

T-2326

A thesis submitted to the Faculty and the Board of Trustees of the Colorado School of Mines in partial fulfillment of the requirements for the degree of Master of Science in Geophysics.

Golden, Colorado

Date April 23, 1980

Signed: Brandon R. Brygider
Brandon R. Brygider

Approved: George V. Keller
George V. Keller
Thesis Advisor

Golden, Colorado

Date April 23, 1980

Phillip R. Romig
Phillip R. Romig
Head of Department

ABSTRACT

During the summer of 1979, a direct current (D.C.) bipole-bipole survey was performed over the Adena oil field in Morgan County, Colorado. The purpose of the survey was to substantiate results reported by House (1979), from the Belle Creek oil field, which suggested that the high resistive oil pay zones could be detected from a surface based D.C. survey. As with the previously reported survey, the D.C. data from Adena were interpreted using a novel approach to enhance the anomaly in the potential field caused by the presence of oil. Where traditional interpretation of apparent resistivities seemed to fail in detecting the anomaly, an approximation of the second vertical derivative of the electric potential was applied to the data. By using methods of interpretation frequently employed by gravity and magnetic potential data analysts, the areal extent and depth to the producing zones were determined.

Based on the similarity of results and success met by these two independent surveys, performed over different oil fields, it is concluded that the second vertical derivative technique is able to enhance and detect the small anomaly in the electric potential produced by a thin oil saturated layer buried at depths equal to at least 1.7 kilometers.

TABLE OF CONTENTS

	<u>Page</u>
INTRODUCTION	1
GEOLOGY	5
THEORY	11
FIELD TECHNIQUE	16
DATA AND DATA REDUCTION	22
APPARENT RESISTIVITY	27
APPROXIMATION OF THE SECOND VERTICAL DERIVATIVE OF THE ELECTRIC POTENTIAL	33
CONCLUSIONS	49
APPENDIX 1 Filtering and Data Files	51
APPENDIX 2 Apparent Resistivity Programs	60
APPENDIX 3 Second Vertical Derivative Program	66
APPENDIX 4 Examples of Filtered Data	69
BIBLIOGRAPHY	75

LIST OF FIGURES

<u>Figure</u>	<u>Description</u>	<u>Page</u>
1	Location map for the Adena oil field, Morgan County, Colorado.	5
2	"J" sand net oil and gas isopach for the Adena oil field.	7
3	Typical geoelectric section at Adena.	8
4	Contour map of the longitudinal resistivity ρ_{L3} in ohm-m for the third geoelectric layer at Adena.	10
5	Model for the determination of the potential at point M due to a point source of current I impressed on the surface of a homogeneous and isotropic earth.	11
6	Plan view of the source and receiver geometry used in the bipole-bipole method.	17
7	Null-lines for the parallel component of the electric field for the N-S and E-W sources. (Base map for station numbering)	21
8a	A sample of the shape of the signal recorded in the field.	23
8b	The form of the matched filter A(I).	23
9	Distances between the source and receiver used to calculate a geometric factor for apparent resistivity.	27
10	Total electric field vector calculation for $ET_{1,3}$ from potential differences V_1 and V_3 , and their associated bipole lengths MN1 and MN2.	29
11	E-W source geometry determination of a geometric factor for the calculation of the total field apparent resistivity.	31

<u>Figure</u>	<u>Description</u>	<u>Page</u>
12	N-S source total field apparent resistivity contour map for the Adena oil field area.	33
13	E-W source total field apparent resistivity contour map for the Adena oil field area.	34
14	Rotated source total field apparent resistivity contour map for the Adena oil field area.	36
2	"J" sand net oil and gas isopach for the Adena oil field.	42
15	N-W source normalized second vertical derivative contour map for the Adena oil field area.	43
16	E-W source normalized second vertical derivative contour map for the Adena oil field area.	44
17	Rotated source normalized second vertical derivative contour map for the Adena oil field area.	45
18	Original signal after filtering by a 3 point averaging filter. Station 40, north bipole receiver, N-S source.	57
19	Original signal after filtering by a matched filter. Station 40, north bipole receiver, N-S source.	58
20	Original signal after filtering by a 3 point averaging filter. Station 15, west bipole receiver, E-W source.	70
21	Original signal after filtering by a matched filter. Station 15, west bipole receiver, E-W source.	71

<u>Figure</u>	<u>Description</u>	<u>Page</u>
22	Original signal after filtering by a 3 point averaging filter. Station 46, south bipole receiver, E-W source.	72
23	Original signal after filtering by a matched filter. Station 46, south bipole receiver, E-W source.	73
24	Original signal after filtering by the matched filter last match. Station 46, south bipole receiver, E-W source.	74

ACKNOWLEDGEMENTS

I wish to express my sincere appreciation to Dr. George V. Keller for his guidance throughout my graduate studies and for his supervision of my thesis, as advisor. My gratitude is also extended to Dr. Catherine Skokan and Dr. Charles Stoyer, for all their many helpful suggestions. For their efforts in the field collecting data, I would like to thank Luke Mamah and Chisengu Mdala. I am indebted to Group Seven, Inc. for loaning me the field equipment and personnel used in collecting data. I also want to thank Sara Wilson for typing my thesis. Finally, I am pleased to acknowledge the Integrated Geophysics Project for providing me with the funds necessary for the completion of my graduate studies and thesis.

This thesis is dedicated to my beloved parents.

INTRODUCTION

The use of electrical prospecting techniques as applied to the exploration for oil began in the early 1920's.

C.A. Heiland suggested that electrical methods might be employed to detect directly the anomaly in resistivity associated with subsurface oil accumulation (Keller, 1968). An electromagnetic approach (called the Eltran Method) using current pulses in a source dipole which are detected with a receiver dipole developed considerable interest in the 1930's. During the course of the 1940's and 1950's new methods using radio-wave frequencies overshadowed the Eltran Method. However, the use of radio-wave methods declined in the 1960's and the present-day explanation of the anomalous response associated with oil fields, is probably due to near-surface affects. In the mid-1960's a wide variety of techniques were being used in the U.S.S.R. to search for oil including the telluric, magnetotelluric, electromagnetic sounding and direct current (D.C.) methods.

From the mid-1960's to the present, Russian investigators have emphasized the use of the magnetotelluric method for reconnaissance, and also employ time-domain transient methods for mapping structure and direct detection of the resistivity anomaly associated with the oil-water contact of oil fields (Kaufman, 1980). In the U.S., the oil industry has not yet seen a significant increase in the use of electrical

techniques in the exploration for oil. However, during the past few years renewed interest in electrical methods applied to oil exploration has resulted in the advent of several transient and D.C. surveys being performed at the Colorado School of Mines. Promising results from a D.C. survey reported by House (1979) have resulted in the author's present work

To further verify that the second vertical derivative method can be used to identify the small anomaly in potential field behavior caused by an oil field, a second survey has been carried out in the vicinity of the Adena field, in the Denver Julesburg Basin (Keller, 1979).

Reviewing the limitations of conventional seismic exploration techniques now being used, in addition to the increasing difficulty with which new oil reserves are being found, it seems appropriate to reconsider the manner in which electrical methods might be applied in the petroleum exploration program. Keller (1968) has suggested three ways electrical techniques might be applied:

- 1) In the search for structures.
- 2) In the search for lithologic changes associated with lithologic oil traps.
- 3) In the recognition of resistivity anomalies associated directly with the presence of oil.

The purpose of this D.C. survey is to verify whether the second vertical derivative method can be used to detect directly the resistivity anomaly producing the distortion in the electric potential associated with the presence of oil in the pore structure of the "D" and "J" members of the

Dakota sandstone in the Adena oil field. Due to the stratigraphic entrapment of oil at Adena (Murry, 1957), additional importance is added to the results of this D.C. survey in the fact that structural control of oil entrapment was insignificant. This fact, coupled with the difficulties encountered by seismic techniques in such areas where stratigraphy controls the entrapment of oil, suggests that similar electrical surveys should be considered as possibly becoming a part of an exploration program.

During the past 30 years the relationship between rock resistivity, fluid content and texture has resulted in the wide use of an empirical relationship, Archie's Law:

$$\rho_r = \rho_w S^{-n} \phi^{-m}$$

where ρ_r is bulk resistivity, ρ_w is fluid resistivity, S is the fraction of pore space filled with fluid, ϕ is the porosity and m and n are empirically arrived at constants. However, we are more concerned with knowing reliable average values of resistivity for a sedimentary section (the so-called geoelectric section) rather than knowing the detailed variation of rock resistivity in response to the factors ρ_w , S and ϕ . With these average values we may begin to evaluate the resolving capabilities of specific surface-based electrical survey techniques (Keller, 1968).

The transverse resistance of a section has been shown to most significantly influence D.C. measurements made on

the surface of a horizontally stratified earth. It is defined to be the sum of the resistances, encountered by a current impressed vertically through a 1m^2 column of rock, contributed by all the layers in the section (Keller, 1977).

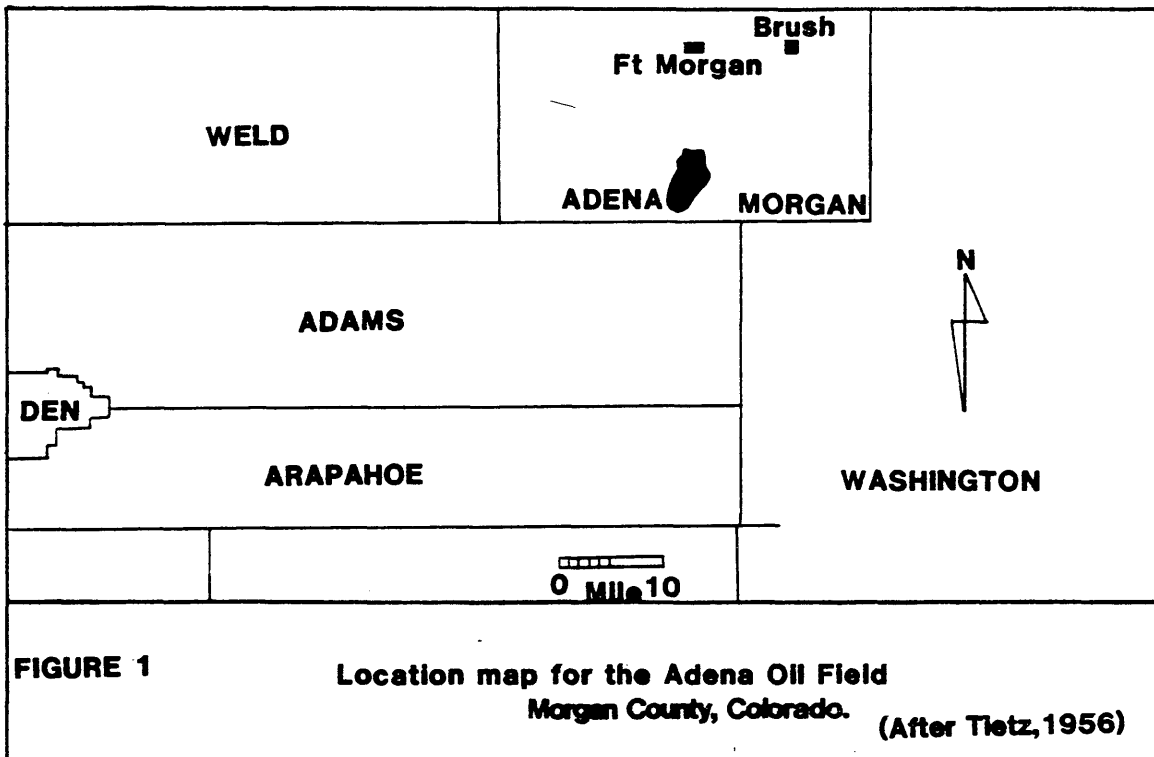
$$T = \sum_{i=1}^m \rho_i h_i$$

where T is the transverse resistance, ρ_i is the resistivity of the i^{th} layer, h_i is the thickness of the i^{th} layer and i is the indice for layers 1 through m .

The ratio of transverse resistance between the pay zone and the overlying section, $T_{\text{oil}}/T_{\text{section}}$, provides a means for determining the ability of an electrical method to resolve the anomaly associated with the pay zone. An oil saturation of 66 percent would increase the resistivity of the pay zone by a factor of 10 compared to the surrounding rock, all other rock properties being equal. The resistivity anomaly measured at the surface with a D.C. method, resulting from such a pay zone, would amount to a few percent depending on relative thicknesses (Keller). The ability to detect such anomalies depends on the magnitude of the anomaly and on the noise inherent with the D.C. method. Because of these resolution difficulties, the second vertical derivative method is used to enhance and identify the small anomaly in potential field behavior caused by the presence of oil.

GEOLOGY

In the early part of 1952 drilling around the Little Beaver Creek Field resulted in locating an excellent stratigraphic type reserve in the upper Dakota "J" sandstone. Wildcatting in Morgan County increased and in May of 1953 the Adena Field was discovered. The Adena Field is the largest in the Denver-Julesburg Basin, located on the gently dipping east flank and near the center of the basin; total production to date is approximately 75 million barrels. Geographically, it is located about ten miles south of the town of Ft. Morgan and is approximately seventy miles north-east of Denver, Colorado (Perry and Overstake, 1955). The location map for the Adena oil field is shown in Figure 1.



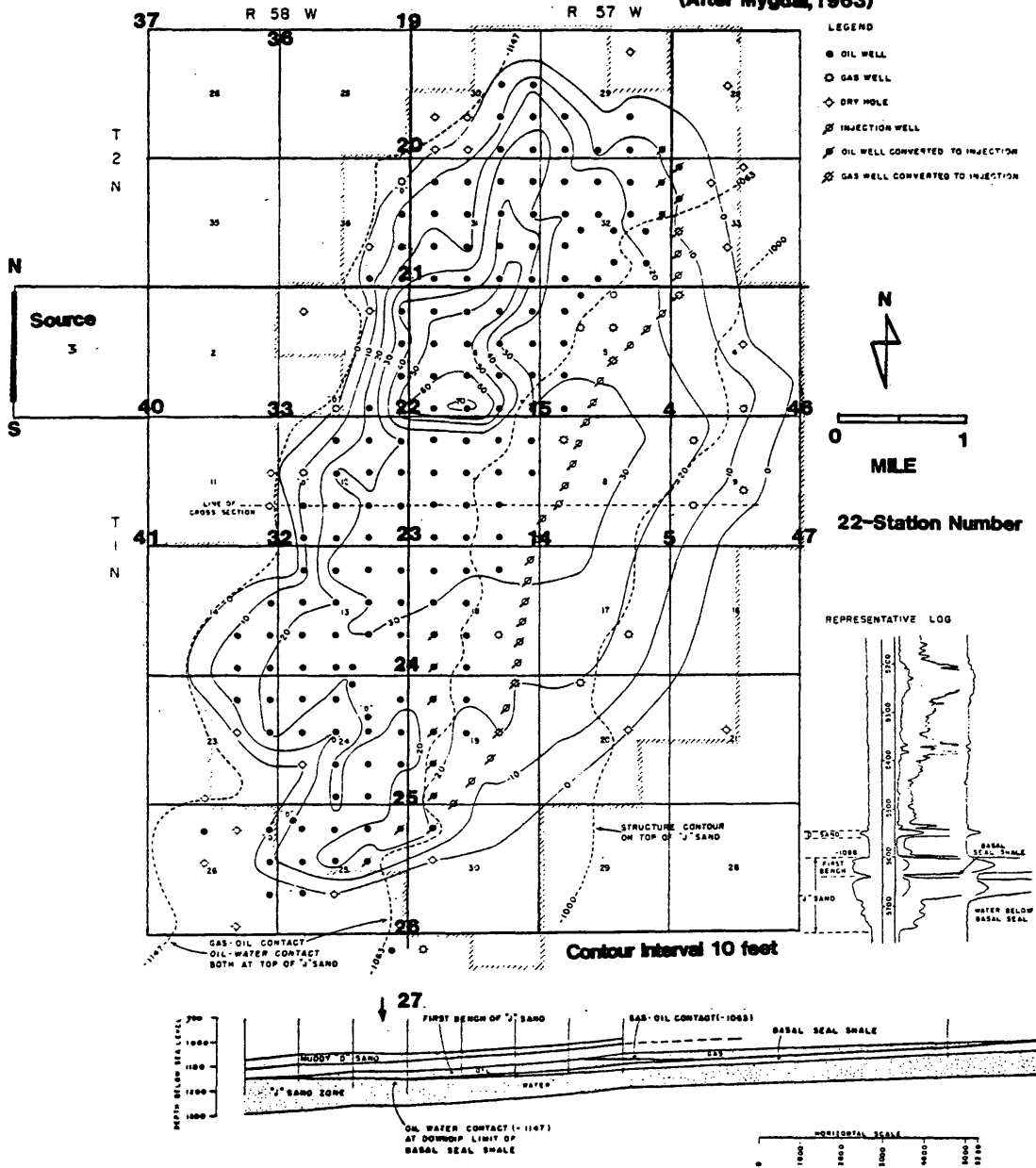
The surface elevation is approximately 4500 feet and the terrain is generally flat. The area extent of the field is 11,425 acres, or seven miles long by four miles wide and the average depth to the pay zone is 5600 feet.

The structure of the basin in the area of the field, including the stratigraphy, is well reported in the literature (Tietz, 1956). The stratigraphic section is normal for the central Denver basin and will be described in terms of its geoelectrically significant layers. The "D" and more important producing "J" sands are members of the Cretaceous Dakota formation.

The "D" sand is composed of fine grained, sub-angular, slightly silty, well consolidated quartz sands interbedded with non-calcareous shales. The sands vary in thickness from zero to 43 feet. The upper and lower contacts of the "D" horizon are conformable. Below the "D" sand, interbedded by shale, is the "J" sand. The "J" sand is fine to medium grained, angular to sub-rounded, well consolidated quartz sand. The uppermost portion of the "J" is productive and varies in thickness from zero to 69 feet and involves conformable deposition (Cullen and Forcade, 1954). (See Figure 2)

The Adena oil field is a good example of a curved barrier trap and is described as a deltaic or off-shore bar sand lens. The barrier encircles the reservoir except on the northwest and is composed of interbedded siltstones and shales. The field has a water drive from the down dip sand with the gas cap butting against the updip barrier. The Dakota sands dip to the west-northwest at approximately

FIGURE 2 "J" Sand net oil and gas isopach for the Adena Oil Field.
(After Mygdal, 1963)



50 feet per mile. Local minor folding does not control production in the "J" sand, but may, to some extent, influence the entrapment of oil in the "D" sands at the north end of the field (Murry, 1957 and Mygdal, 1963).

An extensive well-log study has indicated that the sedimentary section may be divided up into 4 gross geoelectrical layers, as shown in Figure 3.

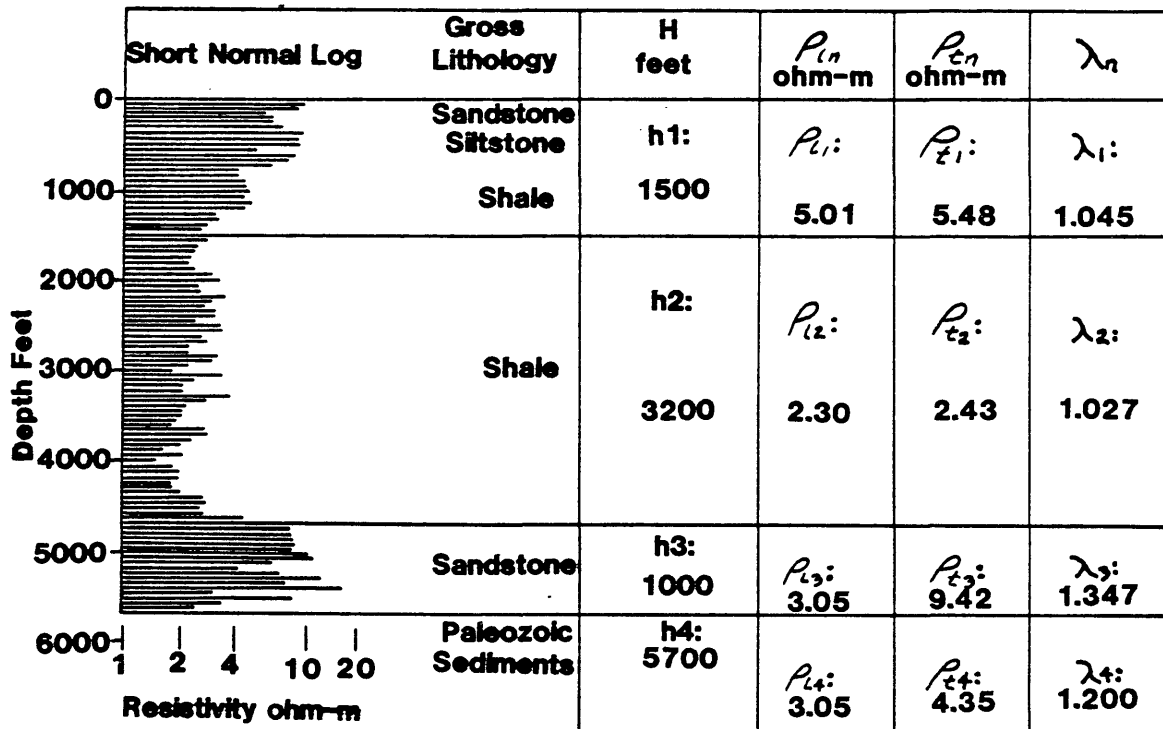


Figure 3 Typical geoelectric section at Adena.
(After Mienardus, 1967)

The base of the fourth layer rests on the Precambrian basement which consists of a complex of schists, gneisses and igneous intrusions. A resistivity of 600 ohm-m is assigned to the basement. The third layer, consisting of the Niobrara, Benton and Dakota formations, is characterized by a range in resistivities from 2 to 10 ohm-m. In the Dakota section of the third layer, the "D" sand produces a 10 foot anomaly of about 20 ohm-m while the first bench of the "J" sand produces a 35 foot anomaly of about 100 ohm-m. These results are based on a representative well log (Meinardus, 1967).

From the original well log study, only the contour map for the longitudinal resistivity of the third layer is available, as shown in Figure 4. Correlation between this contour map and the isopach of the "J" sand, Figure 2, shows an increase in longitudinal resistivity in the area of the thickest portion of the "J" sand. Surface expression of this anomaly can be estimated from a ratio of transverse resistance for $T_{oil}/T_{section}$. This ratio yields a twenty percent anomaly which should be detectable at the surface under ideal conditions.

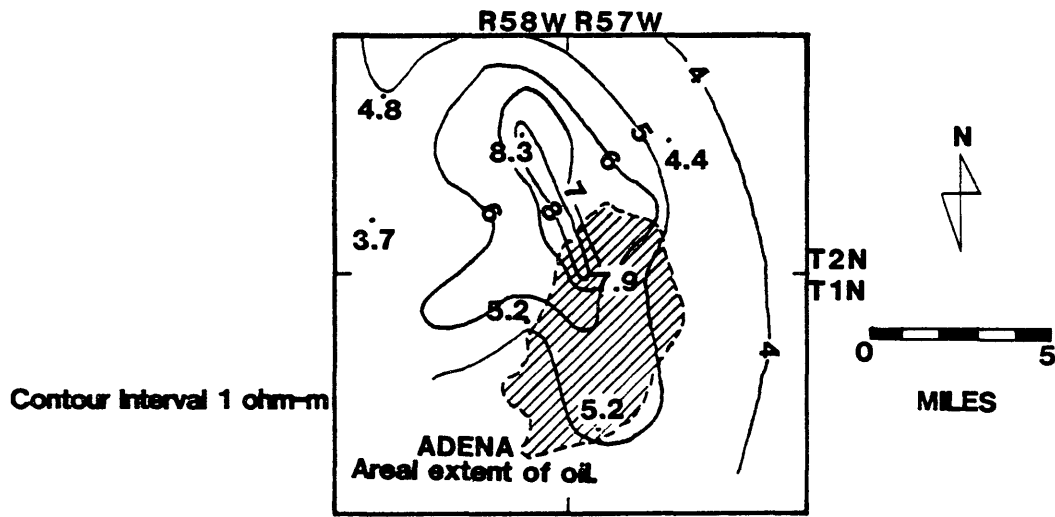


FIGURE 4 Contour map of the longitudinal resistivity ρ_{L3} in ohm-m for the third geoelectric layer at Adena.

(After Mienardus, 1967)

THEORY

The fundamentals of electrical prospecting with direct current are predicated on two basic assumptions, which are used to define the electric potential at a point on the surface of the earth. First, that in a layered sedimentary sequence each of the individual layers is electrically homogeneous and isotropic. Based on the first assumption one can then justify the second assumption which is that Laplace's equation is a valid statement of the behavior of the electric potential in response to the interaction of the impressed current with the earth.

Consider a point source of current I impressed on the surface of the earth as shown in Figure 5.

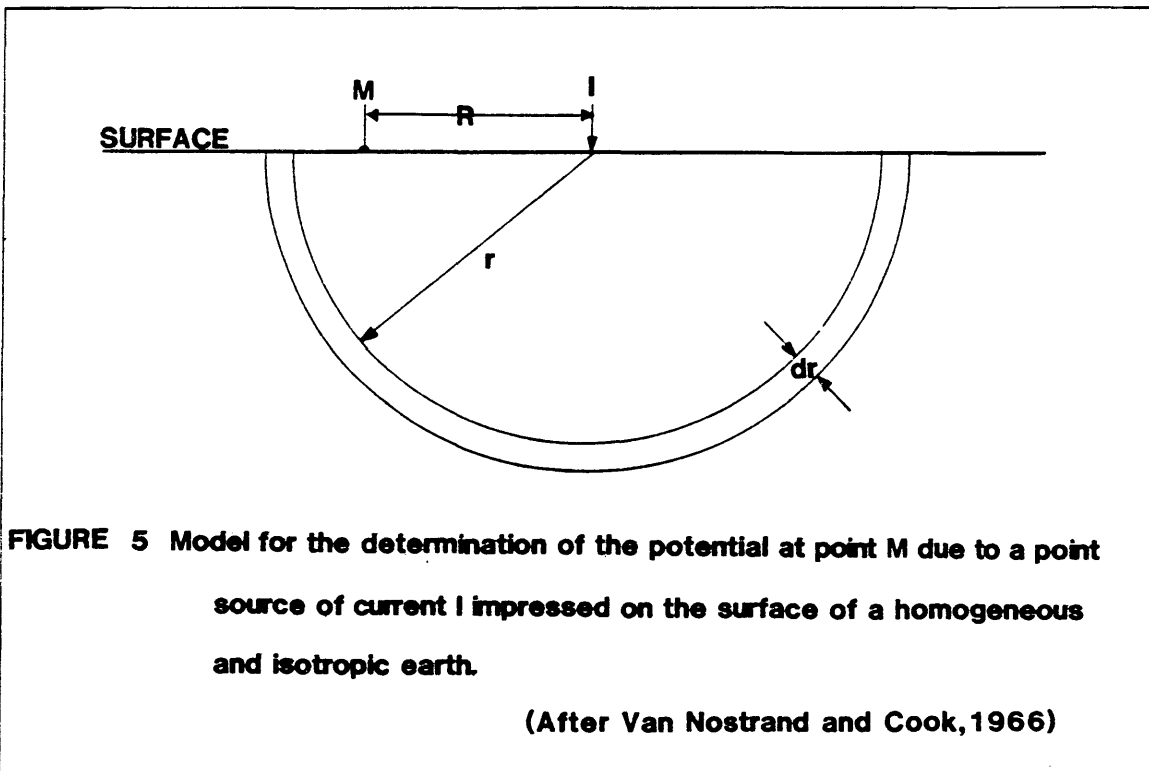


FIGURE 5 Model for the determination of the potential at point M due to a point source of current I impressed on the surface of a homogeneous and isotropic earth.

(After Van Nostrand and Cook, 1966)

The current I flows into an earth with resistivity ρ . It is required to determine the electric potential at point M , a distance R away from the current source. Referencing the potential at point M to the potential at infinity, set the potential at infinity equal to zero. Current flows symmetrically out from the source into the earth. Hence, the current lines are uniformly spaced radial lines and the equipotential surfaces are concentric hemispheres centered at the source. Considering two of these hemispheres at radial distances r and at an infinitesimally greater distance $r + dr$, assume that the flow of current between these hemispheres is linear and therefore apply Ohm's law to describe the behavior of the current. Thus, the potential difference between the inner hemisphere and the outer one is:

$$dU = I \frac{\rho dr}{2\pi r^2}$$

where dr is the length and $2\pi r^2$ the mean cross-sectional area of the linear conductor. To obtain the potential at point M , integrate the above equation from R to infinity:

$$U = \int_R^{\infty} dU = \frac{I\rho}{2\pi} \int_R^{\infty} \frac{dr}{r^2} = \frac{I\rho}{2\pi R}$$

using MKS units, U is in volts (Van Nostrand and Cook, 1966).

In most D.C. techniques the difference in potential measured between two electrodes, M and N, is used in determining the resistivity of the earth: $U_M - U_N = \int_M^N (\vec{E} \cdot d\vec{L})$,

where \vec{E} is the potential gradient along the line connecting points M and N. From this expression, one may compute an "apparent resistivity" for the earth: $\rho_a = K \frac{U_M - U_N}{I}$, where K is a geometric factor which reflects the effect of the source and receiver electrode orientation and I is the current (Alpin, 1950).

The historical development of D.C. methods goes back to the Schlumberger method, invented between 1912 and 1914. At about the same time the Wenner method was also developed. These techniques have now been in use for nearly 70 years, and represent two different approaches to D.C. prospecting. The Wenner array measures potential differences while the Schlumberger array measures the gradient of the potential. In 1950, Alpin reported the use of the Dipole array and with it the third type of electrode arrangement which measures the curvature or second derivative of the potential. During the 1950's the Bipole-Dipole array was seen as a modification of the Dipole array, made by Stefanescu and Doicin, which was used in Rumania for the exploration of oil. Since then, other workers including Risk (Rotating-Dipole array) and Keller (Roving-Dipole array) have altered the traditional array in hopes of improving the D.C. techniques.

Further changes in approach, suggested by Keller, resulted in the bipole-bipole survey technique performed over the Adena oil field. This method combines favorable characteristics of the Rotating-Dipole and Roving-Dipole arrays. These characteristics are the use of two sources to insure good coupling of the current with any anomalous geoelectric bodies and the removal of false anomalies through comparison of the responses from the different sources. Also, rapid deployment and movement of the receiver bipoles favorably characterize this technique, when road access is good.

The bipole-bipole method was used at Adena to detect directly the anomaly in the electric potential field caused by the resistivity contrast between the pay zones and the surrounding media. This anomaly can be viewed as a distortion in the uniform earth electric potential field resulting from the accumulation of a fictitious charge distribution on the interface of the oil saturated layers with the neighboring rock. When the source current produces an electric field vector \vec{E} normal to this interface the charge accumulation is maximized and the source current is said to couple with the pay zone. Thus, the magnitude of the anomaly in the electric potential field should indicate the degree to which a particular source produces a component of the electric field \vec{E} normal to the interface.

Oil producing zones can be modeled using thin high resistive sheets buried in a half-space (Whan, 1979). This approach to modeling led to the use of electric dipoles instead of a charge distribution, in the interpretation of the Belle Creek data reported by House (1979). Interpretation of the Belle Creek data involved the use of an inversion technique in addition to the second vertical derivative calculations. The inversion performed on the Belle Creek data determined the direction and orientation of the dipole moments necessary to model and produce the observed electric potential field. For the interpretation of data collected at Adena the author makes use of an approximation of the second vertical derivative of the electric potential to enhance the anomaly associated with the pay zones.

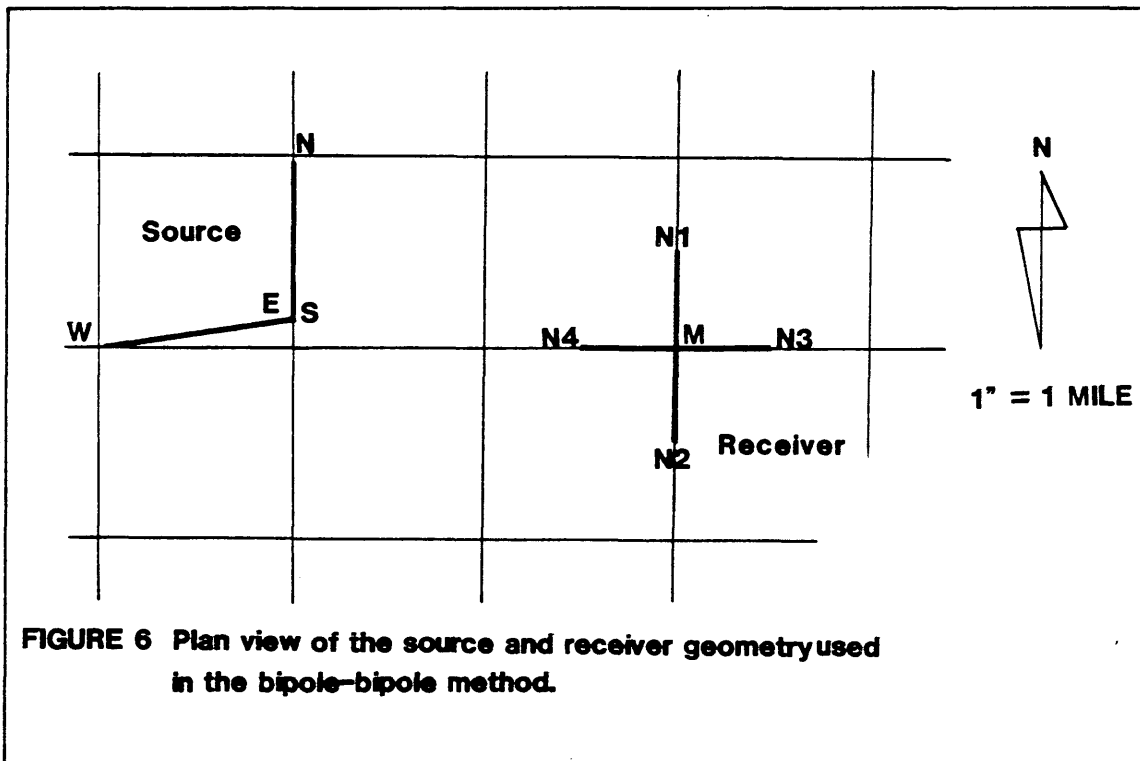
FIELD TECHNIQUE

The Adena oil field is roughly seven miles long and four miles wide, with its long dimension trending southwest to northeast. The average depth to the pay zone, measured from the surface, is 5600 feet. Based on previous geophysical surveys of the field and a well log study of the field, reported by Meinandus (1967), the Adena field was chosen as the site for testing the bipole-bipole method during the summer of 1979.

Two source bipoles were located off of the western edge of the field at a distance roughly equal to twice the depth to the pay zone. This distance was arrived at by considering what the optimum angle of incidence should be to produce a significant current component that would intersect the pay zone vertically. If the sources were located too far off the edge of the field, the current density vector \vec{J} would be horizontal in the vicinity of the pay zone and would not pass vertically through the oil. With the sources on top of the pay zones other problems related to receiving signal too close to the source would arise. The N-S source was 4000 feet long, its south electrode was shared in common with the E-W source whose length was 5100 feet long.

The receiver bipoles were centered at section corners and measurements of the potential differences were

taken along the township and range grid which overlaid the oil field. The common center M electrode was located at the section corner and from this, accurately measured receiver bipoles approximately 2640 feet long (± 20 feet) were laid out along the north, south, east and west section roads. The receiver electrodes N1, N2, N3 and N4 were attached to the ends of the four receiver bipole wires, as shown in Figure 6.



The receiver lengths were made to be approximately one half the depth to the pay zone. This was done in order to subdue near surface effects and to avoid aliasing the broad anomaly in potential produced by the oil. Near surface disturbing potentials will tend to be high frequency and can be averaged using a long sampling interval.

The width of the anomaly resulting from the oil should be a function of the areal extent and depth of the pay zone and thus should be sampled at least twice by the receiver bipoles to avoid aliasing.

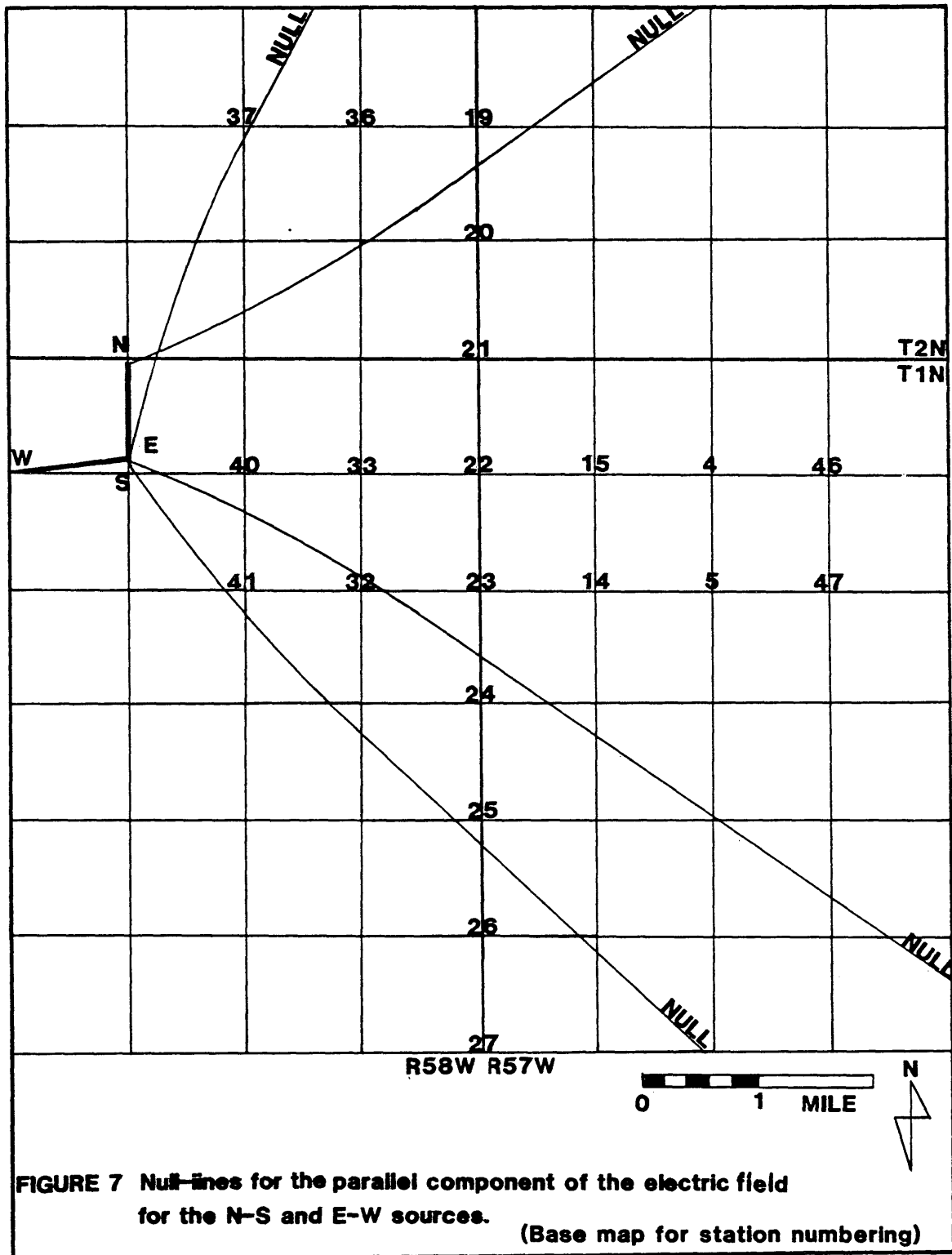
The source truck was located at the common negative B electrode and impressed a square wave current into the ground with a period of 20 seconds negative and 10 seconds positive. The peak to peak current for the N-S source was 150 amps and the peak to peak current for the E-W source was 300 amps. Two culverts and a buried sheet metal plate served as current electrodes. Radio communication was used to request the operator to change from one source to the other. A continuous current record was made in order to determine the switching time and current intensity.

The receiver truck was located at the common M electrode. Once the N-S source began to transmit, the receiver truck recorded the potential difference of the north and south receiver bipoles simultaneously, then switched to recording the east and west bipole potential differences. When the

recording of the N-S source was completed, the source truck was contacted to change to the E-W source and the process of recording potentials was repeated. The bipole potential signal was amplified and also filtered with a 60Hz notch filter. It was then digitally recorded at a half second sampling interval and stored in the memory of a digital field computer, with 12 bit accuracy. The recording time for a receiver record, from any one source, was approximately 8.5 minutes. During this time 14 to 17 signals of the potential difference were stored, each signal length being equal to the 30 second period of the + to - current switching. When the operator was satisfied with the record quality, as seen on a display scope, the entire record was written onto a floppy disk. A color code was used in order to avoid mistakes in identifying the various bipoles. While the receiver truck was recording, a two man team laid out the next station using wire from chest reels and non-polarizing electrodes to make the receiver bipoles. Because of the good road access, the entire procedure of laying out the receiver bipoles, recording and picking up the bipoles could be accomplished within 2 hours.

The most significant problem encountered in the field was the loss of signal when trying to record a null component of the electric field \vec{E} . Null-lines exist at an angle of 54.74° off of the polar axes of a bipole source for a uniform

earth. According to Valla (1979) the variation in null-line location depends on the ratio of the resistivity of the geoelectric section above the basement to the resistivity of the basement. Based on the geoelectric section at Adena the variation in this angle is expected to be from 51.23° at a distance of one mile to 54.74° at distances equal to and greater than ten miles. The locations of the recording stations affected by the null-lines for the parallel component of the electric field for the N-S and E-W sources are shown in Figure 7. For the purpose of determining the second vertical derivative, station components which were affected by null-lines were assumed to yield a potential difference equal to zero. Other major problems which reduced the number of interpretable stations involved the distorting effects produced by pipelines and the noise associated with power lines.



DATA AND DATA REDUCTION

Due to time limitations and equipment breakdown, only 21 out of the desired 47 stations were recorded. Ultimately, even these 21 stations were reduced to 14 interpretable stations for the N-S source and 16 stations for the E-W source. Problems related to the effects of null-lines, pipelines and power lines were seen to be principally responsible for the poor record quality. However, beginning with the original field data, 85 records, each having two channels of received signal, were first plotted using a 3 point averaging filter to smooth out or alias the high frequency noise. The next step was to measure the peak to peak offsets of the 14 to 17 signals present on any one channel of a record. The problem of how to filter the data caused a major delay in the reduction of data. After trying two approaches to filtering which failed, the author filtered the digital field data using a matched filter approach often used in seismic processing, as suggested by Dr. Charles Stoyer (1980).

The field data were examined for all of the stations recorded. The period of switching polarity from positive to negative was determined and was found to be very consistent, with the exception of a few records. The objective of the filtering was to determine the peak to peak offset of the potential difference measured in the field, after

the signal had been multiplied by a gain factor, and to reduce the effect of telluric noise. The shape of the received signal was a rounded square wave as shown in Figure 8a. The matched filter that was convolved with the received signal was designed to be as close a representation of the original source signal as possible. From the original signal sampling rate of .5 seconds recorded for 30 seconds per signal period, the following sixty matched filter coefficients were used: $A(I) = -1.90$ for $I = 1,10$; $A(11)$ and $A(50) = 0.0$; $A(I) = 1.00$ for $I = 11,49$ and $A(I) = -1.90$ for $I = 51,60$. The final shape of the matched filter is shown in Figure 8b.

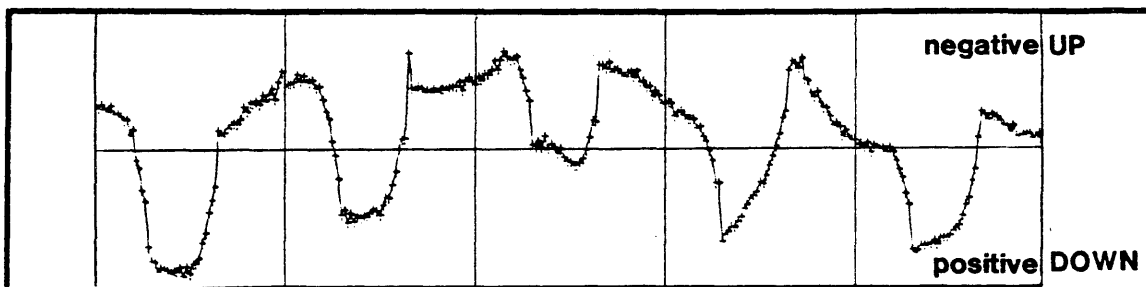


FIGURE 8a A sample of the shape of the signal recorded in the field.

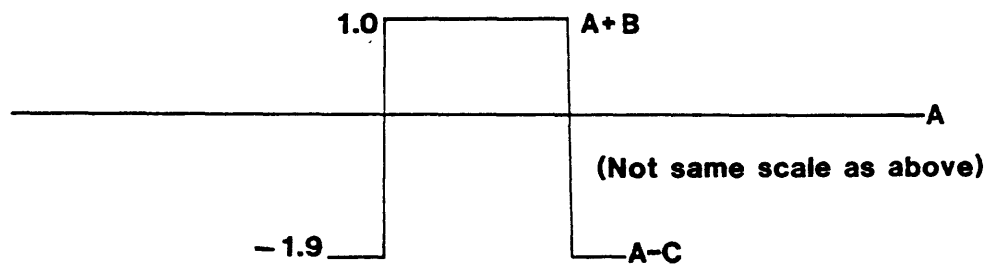


FIGURE 8b The form of the matched filter $A(I)$.

To obtain the offset (b+c) the following calculation is performed:

$$\begin{aligned} 38(1.0)(b+a)-20(1.90)(a-c) &= \\ &= 38b+38a-38a+38c = 38b+38c. \end{aligned}$$

Division by the number of sample points, $\frac{38b+38c}{38} = (b+c)$, yields the offset. The assumption of the coefficients A(11) and A(50) being set equal to zero was determined to yield a more accurate value for the true offsets in the original data than using a filter without these transition points. Several test cases were examined which show that a filter with these transition points somewhat removed the distorting effects produced by the rounded nature of the received signal. This matched filter was then convolved with the field data. The filter programs, an example of the matched filter output and an example of the 3 point averaging filter output appear in Appendix 1. A comparison between the offset obtained by hand from the field data, with the offset produced by the matched filter show a negligible difference. However, the time required to determine the offset from the matched filter output was less than the time necessary to determine the offset by hand. In some instances, when the signal was especially noisy, a matched filter composed of three square waves was convolved through the data. This longer filter helped to average out the noise in especially poor records, but reduced the number of interpretable offsets due to a longer filter on lap.

By recording N signals and stacking, the random noise level should be reduced by a factor of $(N-1)^{\frac{1}{2}}$ (Keller, 1969). For N=17, the noise is reduced by a factor of 4. In a few records only 4 signals were interpretable and thus the noise level was only reduced by a factor of $(3)^{\frac{1}{2}}$. This stacking coupled with accurate bipole locations and lengths should increase the reliability of the survey results.

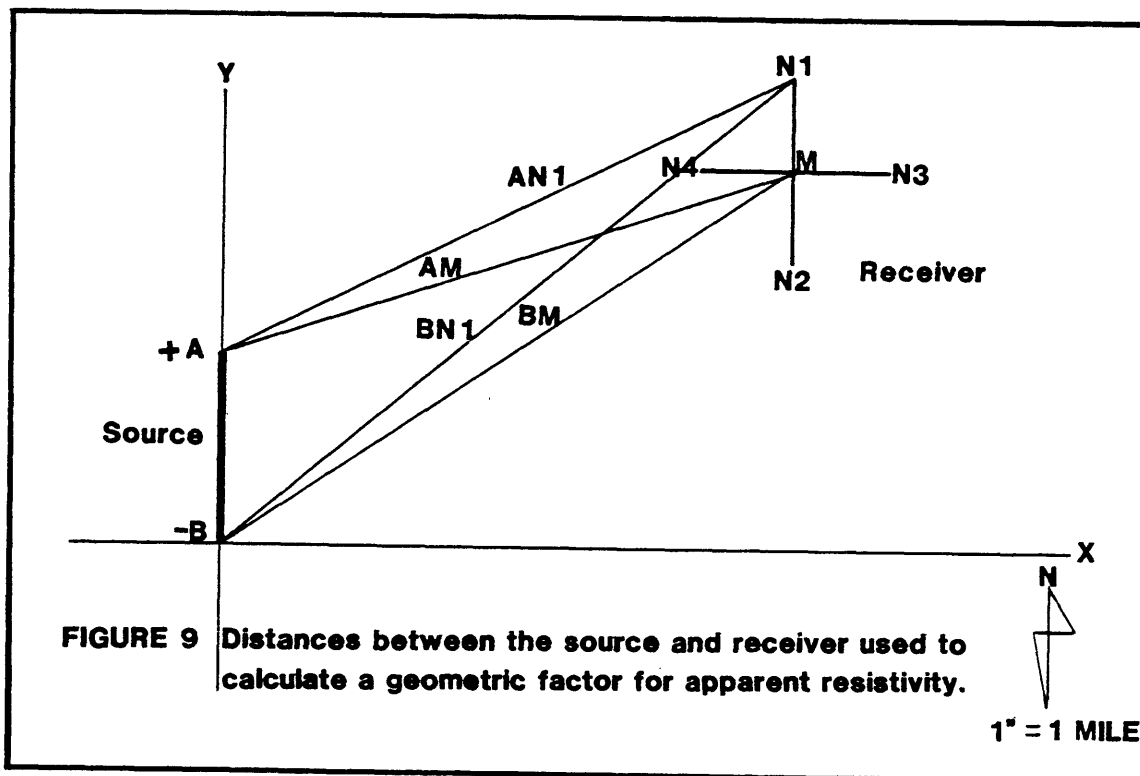
After all the stations were interpreted, a sign convention was adopted based on the arbitrary decision to make the common B electrode of the two sources negative with the north and west electrodes alternately being positive. Also, the common M receiver potential electrode was assigned a negative sign and all other N electrodes were positive. Then, depending on whether the four \vec{E} field vectors of the receiver were opposing or in the same direction as the current density vector \vec{J} of a particular source, the sign of the \vec{E} field vectors would be either negative when opposing or positive if both \vec{E} and \vec{J} were in the same direction.

Finally, the base map for the oil field was digitized and all distances converted to meters. Then two data files for the two sources were created and appear in Appendix 1. Both files contain the following information for each station interpreted: the coordinates of the M electrode, the coordinates of all four N electrodes associated with the common M electrode, the respective potential differences

normalized by a gain factor and the average current impressed into the ground while the N-S and then the E-W receiver bipole pairs were being recorded.

APPARENT RESISTIVITY

Since the electric potential is a scalar function its addition is governed by the law of superposition. Based on this, consider the potential measured at the receiver electrode M and any of the four N electrodes as four separate sets of bipole potential differences resulting from the source electrodes +A and -B. An example of the potential as measured at electrodes M and N1 is shown in Figure 9. From the section on theory, the expression for the potential on the surface of a homogeneous and isotropic earth resulting from a point current source is $U_M = \frac{\rho I}{2\pi} \frac{1}{r}$. Then using the



law of superposition, the expressions for the potential at electrodes M and N1 are: $U_M = \frac{\rho}{2\pi} \frac{I}{AM} - \frac{I}{BM}$ and $U_{N1} = \frac{\rho}{2\pi} \frac{I}{AN1} - \frac{I}{BN1}$. Taking the difference of potential between U_M and U_{N1} and inverting the equation for ρ , yields:

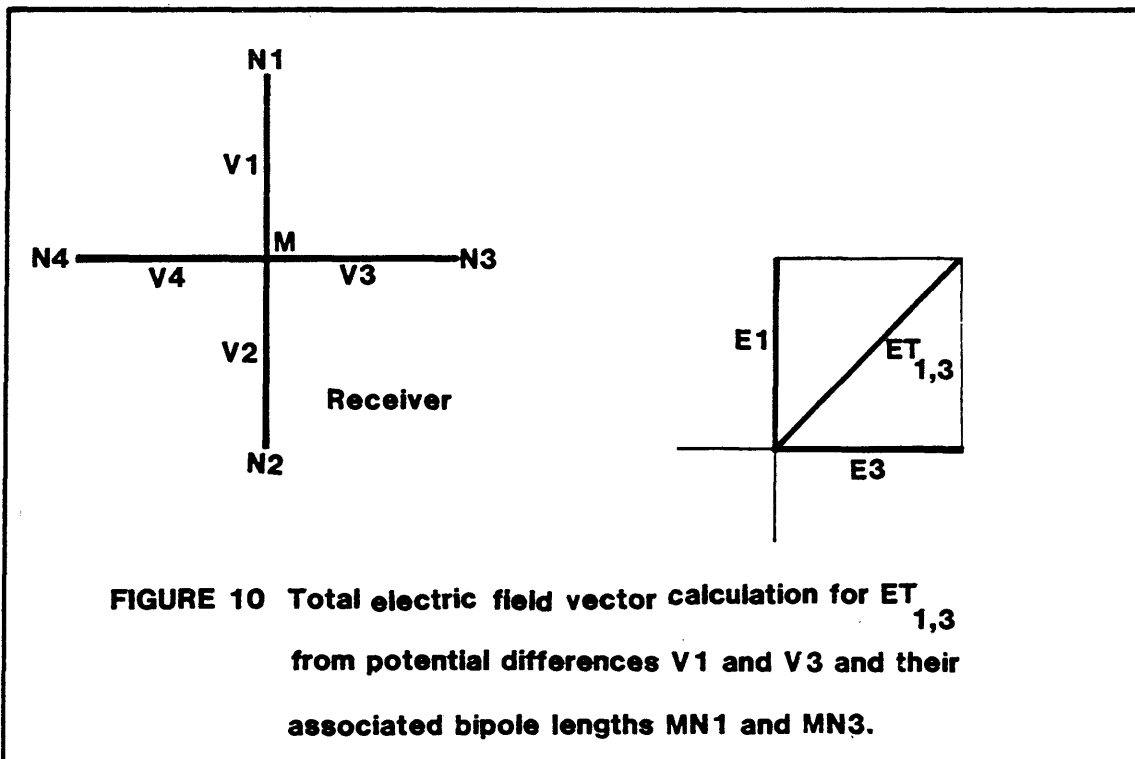
$$\rho = \frac{U_M - U_{N1}}{I} \left[\frac{2}{\frac{1}{AM} - \frac{1}{BM} - \frac{1}{AN1} - \frac{1}{BN1}} \right]$$

This equation may be used to determine the true resistivity of the earth only when the earth is completely uniform. If the earth is not uniform, this equation may be used to define a quantity called the "apparent resistivity" of the earth (Keller, 1966).

The formula was used to compute the apparent resistivity for stations at distances less than five times the receiver bipole lengths, as measured from the center of each source. Four apparent resistivities were calculated at each station in lieu of the four receiver bipoles. These values of apparent resistivity were then averaged and plotted at the center of the respective station. Since there were a limited number of stations at which this method for determining apparent resistivity was used, no contour maps of these values were prepared. The computer program for the apparent resistivity appears in Appendix 2.

At distances, as measured from the center of the sources, greater than five times the bipole receiver lengths the total field apparent resistivity is determined (Keller, and others,

1975). In this case, the receiver bipoles approximate dipoles and the development and formulas for bipole-dipole total field resistivity apply. This approximation is based on the premise that the electric field is being measured at a given station. The electric field component \vec{E}_1 , along the direction of the measuring dipole MN1 is then calculated by: $\vec{E}_1 = \frac{U_M - U_{N1}}{MN1}$, where $U_M - U_{N1} = V1$ is the potential difference and MN1 is the dipole length. Total electric field vectors $ET_{i,j}$ were then arrived at by vector addition of any two adjacent electric field components produced by the four dipole receivers. This procedure resulted in the calculation of four total electric field vectors for each station from any given source as shown in Figure 10.



Next, the source and receiver geometry for calculation of a geometric factor in apparent resistivity determination was developed after Zohdy (1978). Total field apparent resistivity ρ_a is calculated using the formula:

$$\rho_a = \frac{2\pi ET}{I} \left[\frac{1}{\left[(YA/AM^3 - YB/BM^3)^2 + (XA/AM^3 - XB/BM^3)^2 \right]^{1/2}} \right]$$

where:

AM is the distance from the positive electrode of the source to the center M electrode of the station,

BM is the distance from the negative electrode of the source to the center M electrode of the station,

XA is the X distance from the positive electrode to the center of the station,

YA is the Y distance from the positive electrode to the center of the station,

XB is the X distance from the negative electrode to the center of the station,

YB is the Y distance from the negative electrode to the center of the station,

I is the current and ET is the total electric field vector.

The geometry of the source and receiver for the determination of the geometric factor is shown for the E-W source in Figure 11.

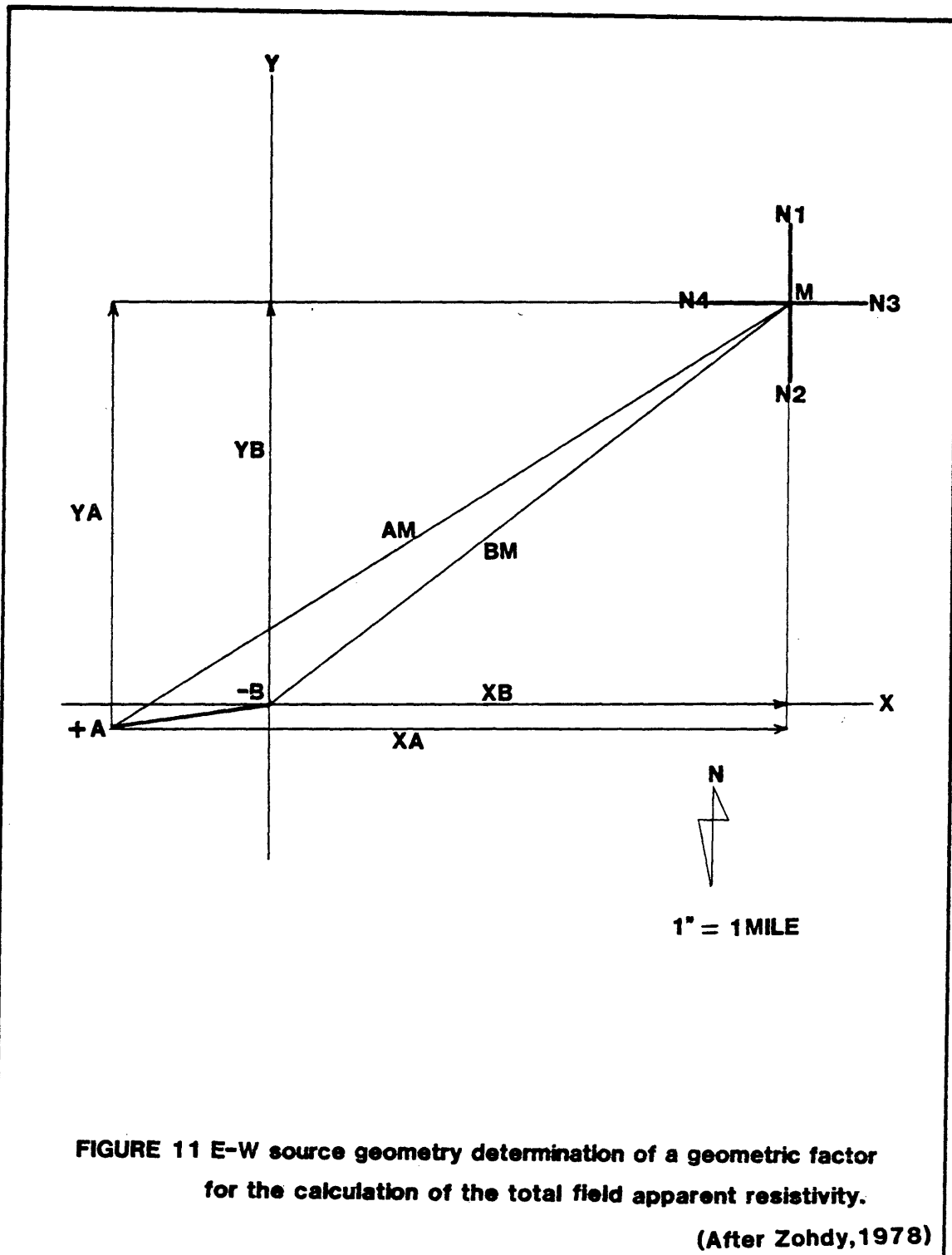
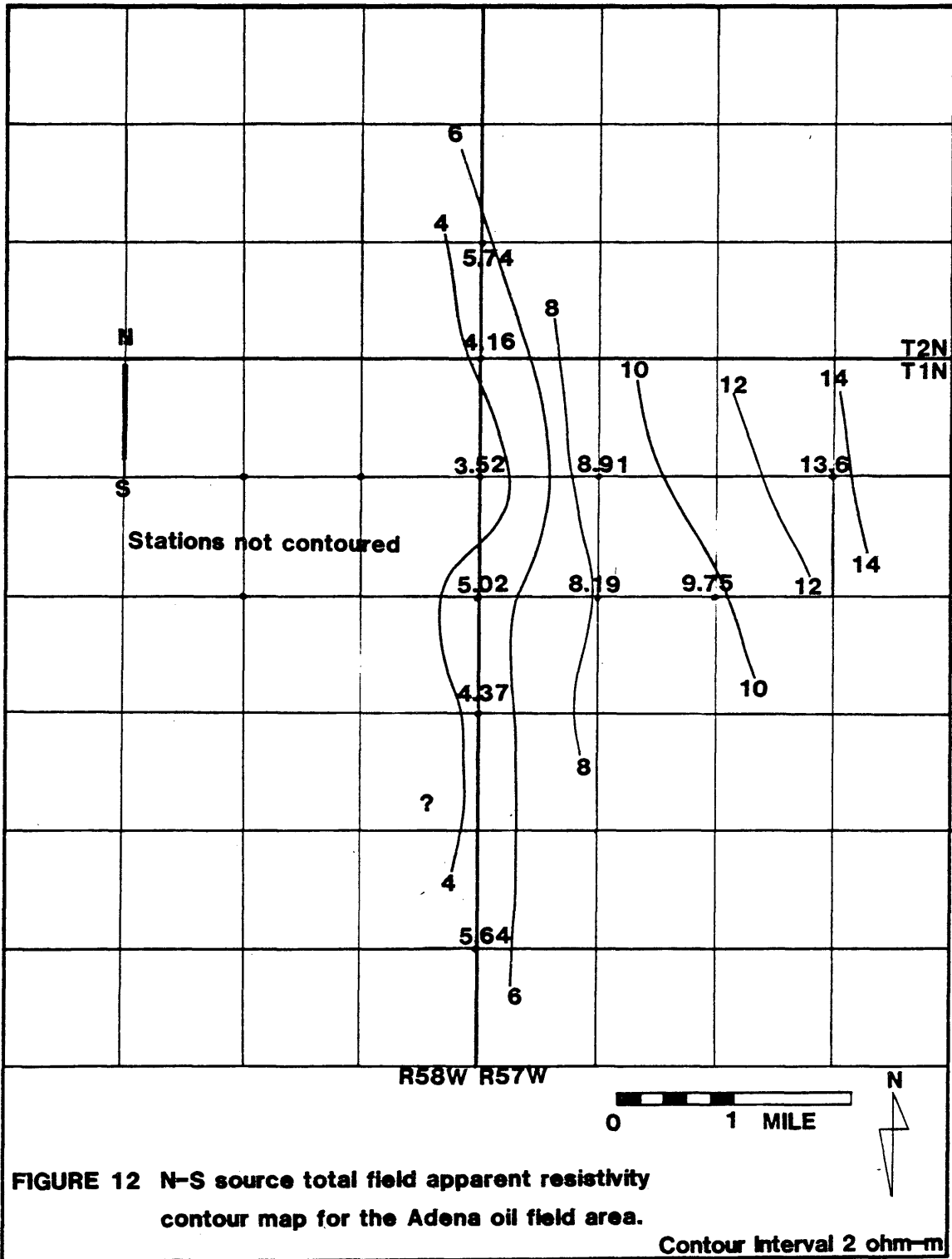


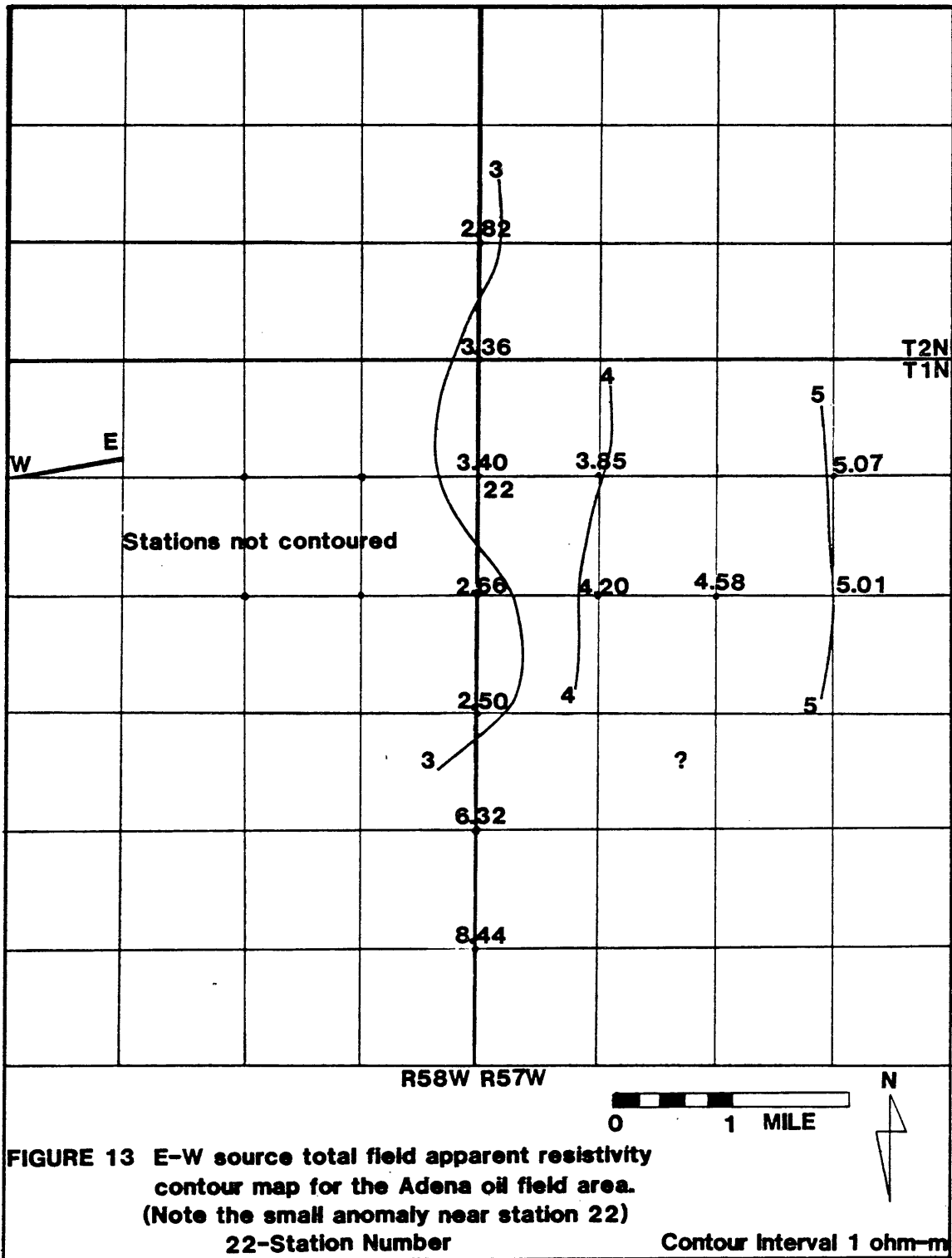
FIGURE 11 E-W source geometry determination of a geometric factor for the calculation of the total field apparent resistivity.

(After Zohdy, 1978)

Four total field apparent resistivities were calculated at each station. These values were averaged and the averaged apparent resistivities plotted at the center of each station and contoured. The apparent resistivities calculated for distances less than five times the bipole lengths were not plotted on these maps. This was because of their poor correlation with the total field apparent resistivities which reflects the differences in the two geometric factors used in the different formulas used to calculate the two apparent resistivities. The contour maps of total field apparent resistivity for the N-S and E-W sources appear in Figures 12 and 13, respectively. The computer program for total field apparent resistivity also appears in Appendix 2.

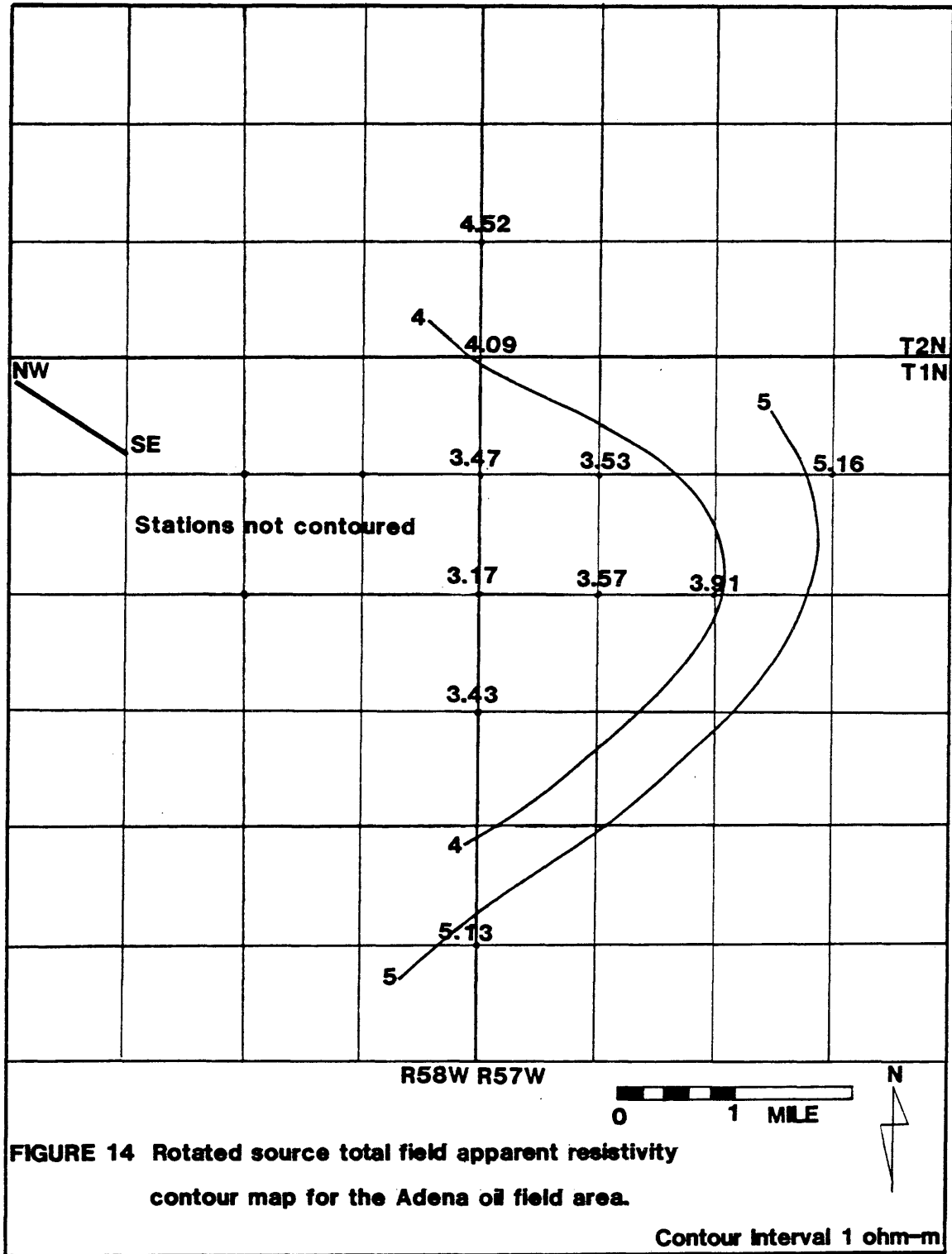
Generally speaking, one may make a comparison between these apparent resistivity maps and the theoretical pattern of apparent resistivity for the case of a single layer resting on an insulating basement (Keller, and others, 1975). The comparison shows the following similarities; that values of apparent resistivity near the polar axis of a source are relatively low and that with increasing distance from the source the apparent resistivity also increases. As for being able to detect any anomaly resulting from the resistive pay zone, no apparent anomaly shows up on the N-S source (Figure 12). However, on the E-W source (Figure 13) the small anomaly around station 22 does in fact





correspond with the thickest portion of the pay zone as seen in Figure 2. This tendency for the E-W source to show an anomaly is probably related to the E-W source coupling with the pay zone to a higher degree than the current from the N-S source. If this can be interpreted as an anomaly, then the sensitivity of the bipole-bipole survey was such that it detected the twenty percent anomaly expected from calculations of the ratio of transverse resistance between the overlying section and the pay zone.

For those stations interpretable from both sources, a fictitious rotated current source was created by vectorially adding the N-S and E-W current sources. The potential differences measured at each station from the original current sources, were added together to produce potential differences for the rotated source. The rotated current intensity was calculated by squaring, summing and taking the square root of the respective currents associated with the original sources. Apparent resistivities were then calculated using the same approach as before and a contour map for the rotated source apparent resistivity appears in Figure 14. This apparent resistivity map does not seem to contradict the anticipated variation in apparent resistivity expected from the theoretical apparent resistivity model. However, no anomaly appears on this contour map and this may suggest that coupling of the fictitious current is again not as good as that produced by the E-W source.



In review of the results from the apparent resistivity contour maps one must acknowledge the fact that if an anomaly is detectable it is very slight and is not confirmed by the other sources. This suggests that the slight anomaly noticed on the E-W source is debatable and thus would probably not stand alone as evidence of being able to detect the pay zone using the traditional approach to interpretation of D.C. bipole-bipole data. However, this does not preclude the use of a non-traditional approach to the interpretation of D.C. bipole-bipole data in order to enhance any anomaly in the potential field produced by the oil.

APPROXIMATION OF THE SECOND VERTICAL DERIVATIVE
OF THE ELECTRIC POTENTIAL

It has been shown that there are definite limitations to resolving thin high resistive bodies at depth based on the interpretation of apparent resistivity data. This fact leads us to consider another technique which should be more sensitive to the distortion of the potential field. The distortion of the primary potential field may be viewed as a result of an imaginary charge distribution arising on the interface between the surrounding media and the higher resistive oil saturated layer, when current is impressed across this interface. To detect this distortion in the potential field, the second vertical derivative of the electric potential, which is a measure of the curvature of the field, is approximated and examined to see whether this technique can enhance the anomaly produced by the oil layer.

This approach, which enhances the small anomaly in electric potential resulting from the oil, is predicated on work done by Evjen (1936), Henderson and Zietz (1949) and by Peters (1949) in the field of interpretation of gravity and magnetic potentials. Common characteristics shared by the magnetic, gravitational and electric potentials - such as being conservative fields whose behavior is defined by Laplace's equation - allow for the application of a basic theoretical approach to the electric potential. One of the

methods of enhancing potential data is downward continuation, another method is that of calculating various derivatives and making contour maps of the derivative values. Smaller anomalies in potential are often identifiable by a change in the curvature of the potential field and curvature evaluation depends largely on the second derivative (Peters, 1949). Evjen (1936) demonstrated the higher resolving power of the first vertical derivative, but even greater resolution is afforded by the second vertical derivative of the field.

The second derivative of the electric potential was approximated at each station using its four bipole receivers. The development of this approximation follows from the assumption that the field is stationary. For the field to be stationary one must require that there is no net charge accumulation within the region of study and that the variation in frequency of current be low enough to assume direct current. Then, Laplace's equation is a valid statement of the behavior of the electric potential and may be written as:

$$\nabla^2 U = \frac{\partial^2 U}{\partial X^2} + \frac{\partial^2 U}{\partial Y^2} + \frac{\partial^2 U}{\partial Z^2} = 0$$

with the second vertical derivative being:

$$\frac{\partial^2 U}{\partial Z^2} = - \left[\frac{\partial^2 U}{\partial X^2} + \frac{\partial^2 U}{\partial Y^2} \right].$$

The electric field intensity \vec{E} , is the first derivative of the electric potential along the direction of the receiver bipole and may be defined as: $\vec{E}_1 = \frac{V_1}{MN_1}$. Here, V_1 is the difference in potential between the two electrodes of the north bipole and MN_1 the length of this bipole. If the first derivative of the electric potential of the north bipole \vec{E}_1 is subtracted from the derivative of the south bipole \vec{E}_2 and if this difference is divided by the average of their respective bipole lengths MN , then an approximation of the second derivative of the potential in the direction of the bipoles has been determined:

$\frac{E_1 - E_2}{MN} \approx \frac{\partial^2 U}{\partial Y^2}$, where Y is taken to be in the direction south to north and the X direction is west to east. Similarly the approximate second derivative in the X direction is:

$$\frac{E_3 - E_4}{MN} \approx \frac{\partial^2 U}{\partial X^2}.$$

Then, returning to the definition of the second vertical derivative the final result is:

$$\frac{\partial^2 U}{\partial Z^2} = - \left[\frac{E_1 - E_2}{MN} + \frac{E_3 - E_4}{MN} \right].$$

The advantage to determining the second vertical derivative rather than the potential itself, or the first derivative measured in terms of components of the electric field can be seen from model studies (Whan, 1979). For a point source of current, I , in a uniform earth with resistivity, ρ , the second vertical derivative of potential is:

$$\frac{\partial^2 U}{\partial Z^2} = \frac{-\rho I}{2\pi r^3} + \frac{3Z^2 \rho I}{2\pi r^5}.$$

For measurement at the earth's surface the second term is zero. The important fact shown by this expression is that the second vertical derivative decreases as the distance cubed, rather than as the distance to the first and second powers, as is the case with potential and electric field, respectively. This provides the possibility that it may be possible to detect the contribution to determinations of the second vertical derivative from a subsurface target zone more easily than if measurements of electric field or potential are made (Keller, 1979).

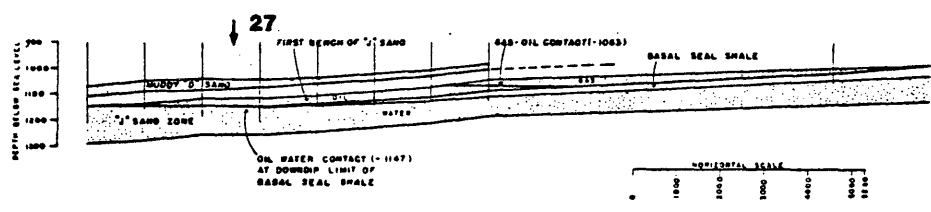
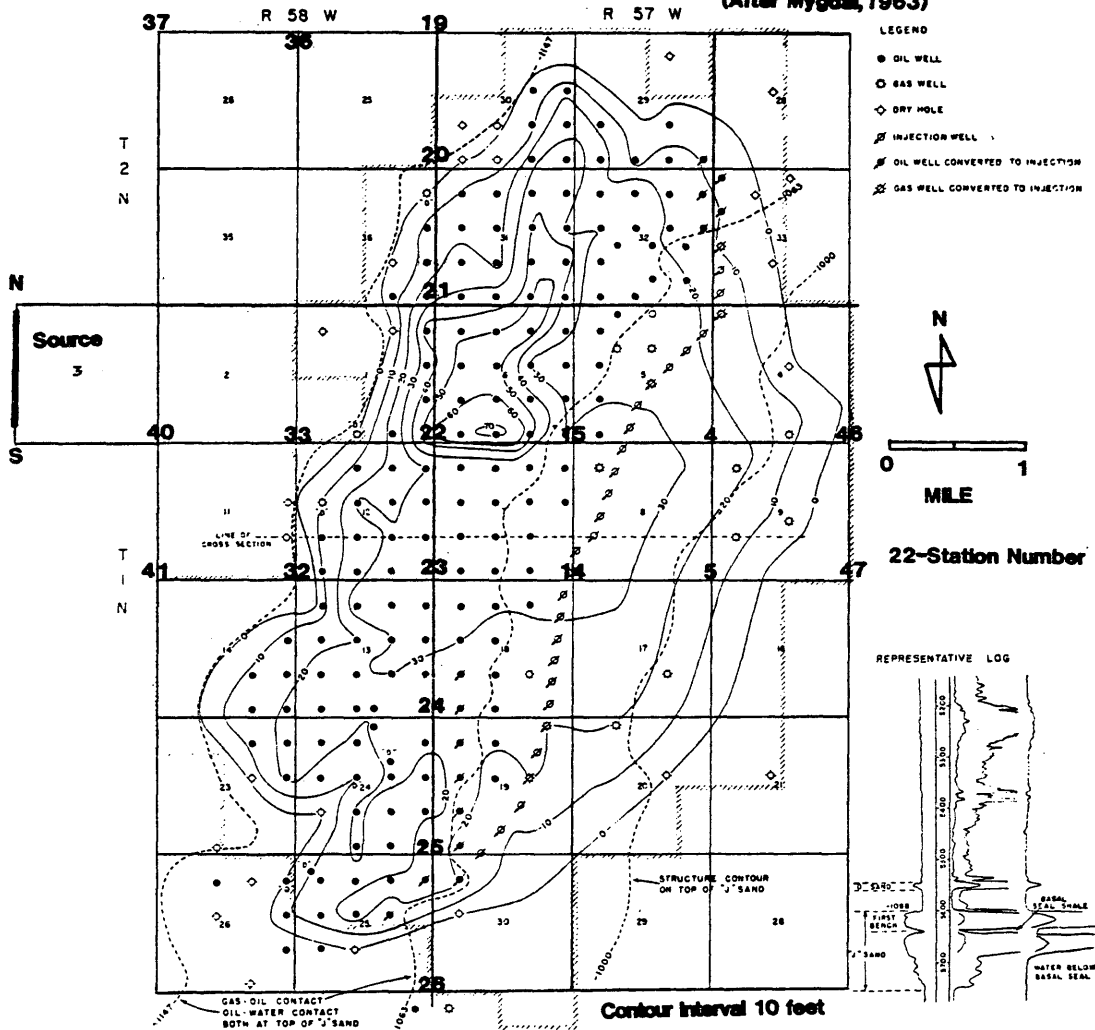
Once the second vertical derivative was approximated from the N-S, E-W and rotated sources, these derivative values were normalized by the theoretical second vertical derivative of a uniform earth with resistivity $\rho=1$. This was done to remove the influence of the curvature of the primary field and enhance the distorting influence of the secondary potential due to the presence of oil. The computer program for the determination of the uniform earth second vertical derivative appears in Appendix 3.

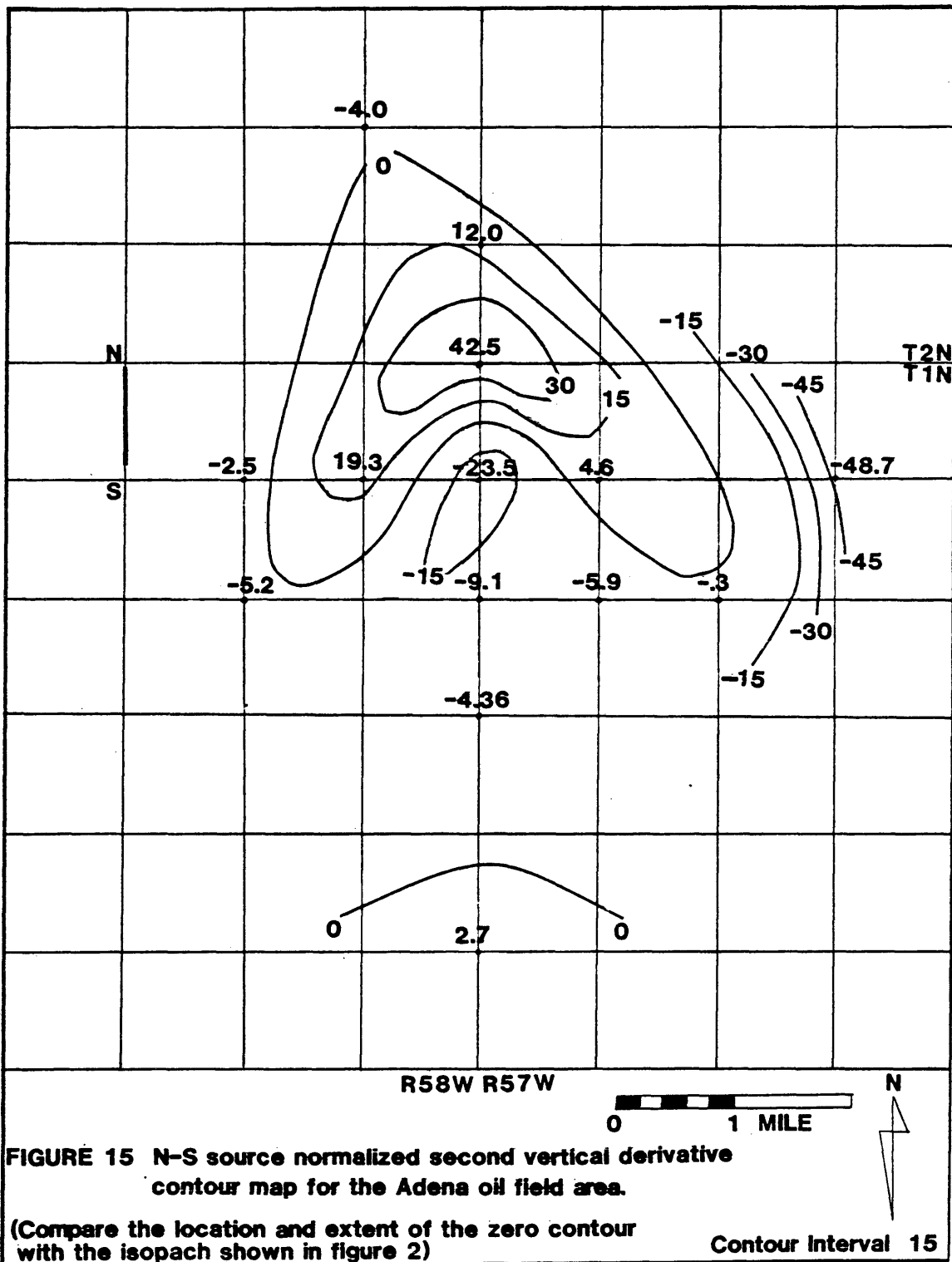
For easy comparison between the results of the three source second vertical derivative contour maps and the pay zone isopach, Figure 2 is reproduced on page 42. Then appearing after the isopach are the three source second vertical derivative (SVD) contour maps normalized by the uniform earth SVD, shown as Figures 15, 16 and 17, respectively.

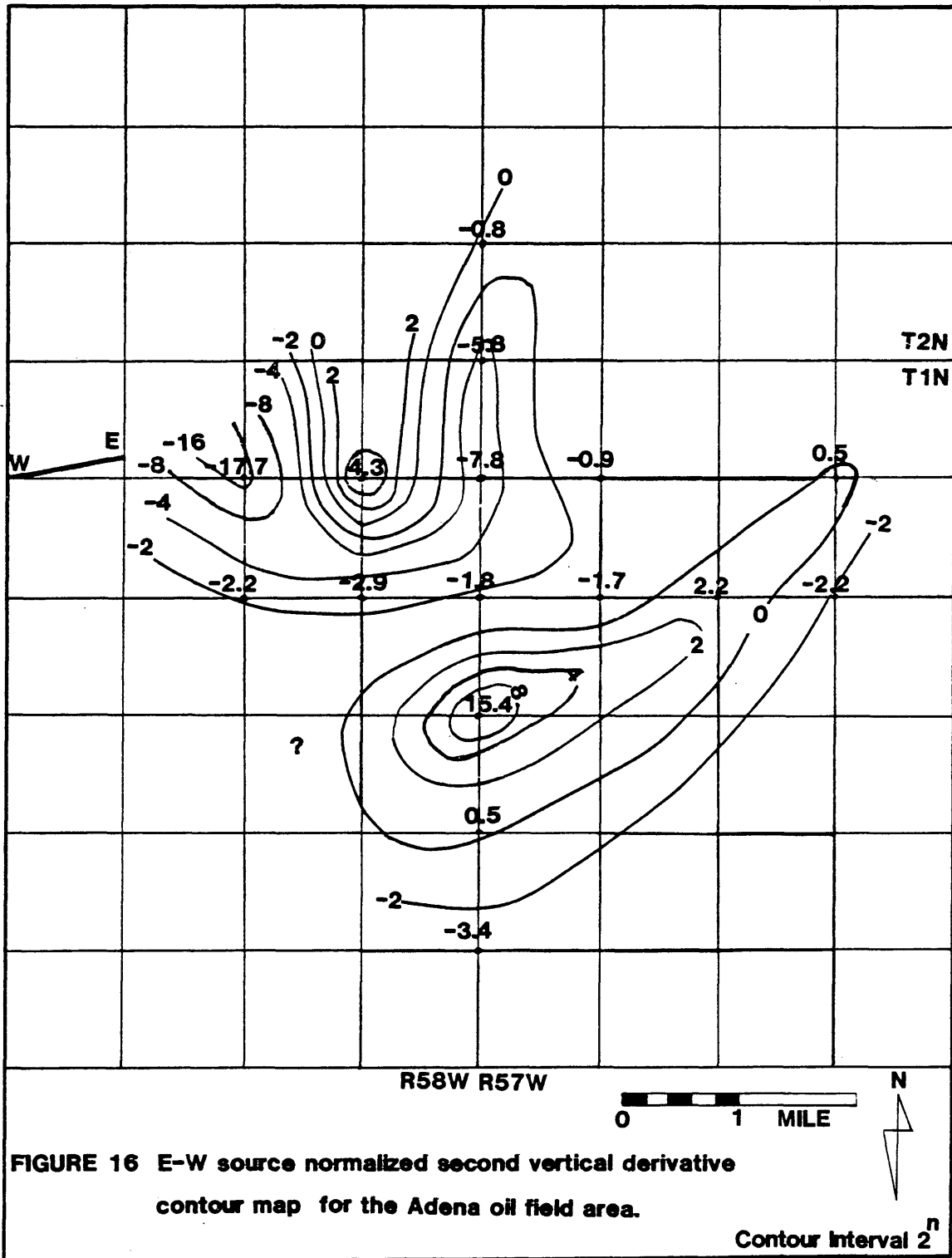
The interpretation of these contour maps is qualitative in nature. However, quantitative interpretations of airborne magnetic data are most often performed and entail

FIGURE 2 "J" Sand net oil and gas isopach for the Adena Oil Field.

(After Mygdal, 1963)







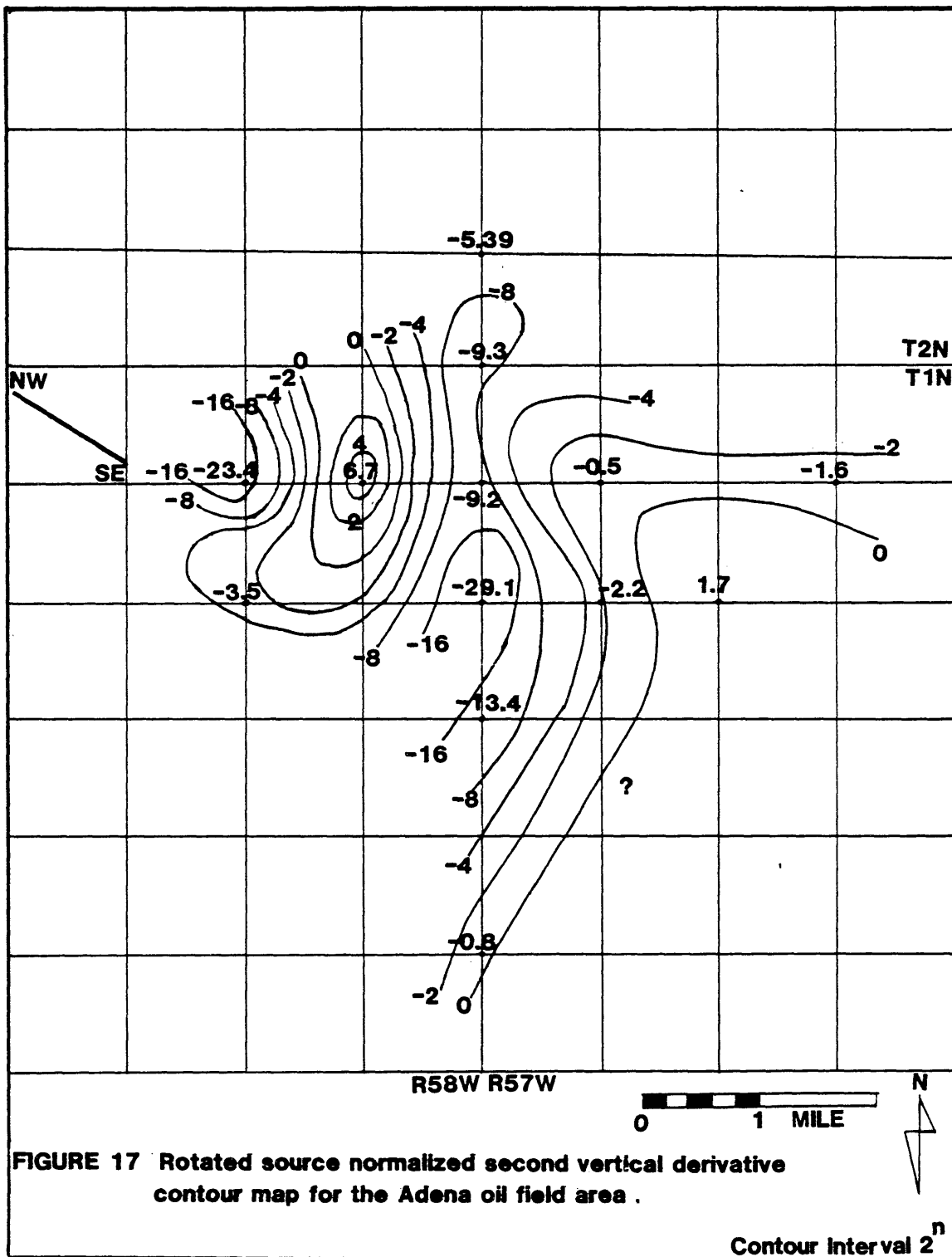


FIGURE 17 Rotated source normalized second vertical derivative contour map for the Adena oil field area .

Contour Interval 2^n

relatively complex methods for depth determination. Yet, similar general techniques and results may be used in the interpretation of the SVD electric potential contour maps. Important characteristics of these SVD values for interpretation purposes involve the zero crossings and width of the positive anomalies observed on the contour maps. Interpretation of the SVD values depends on the ratio of the observed electric potential field to the primary potential field. The observed potential field is composed of the current source primary field and the distorting secondary field produced by the accumulation of a charge distribution on the surface of the pay zone. Normalizing the observed field with the primary field for a uniform earth removes the effect of the decay in magnitude of the primary field as the distance away from the source increases. This allows the interpreter to compare a SVD value at a specific location with a value at any other point in the survey area.

The density of the charge distribution should be greatest on the edge of the pay zone closest to the source, in response to the relative magnitude of the primary field. Because these charges produce the secondary potential field, the anomaly in the SVD values is expected to shift towards the source relative to the actual location of the thicker portions of the pay zone. A limiting depth may be determined based on the half width of the closed zero contour if it is

assumed that the high density charge distribution producing this anomaly, is considered to approximate a sphere (Keller, 1980). However, the influence of the remaining edge of the pay zone away from the source still effects the observed field. This will tend to increase the areal extent of the closed zero contour to the point that it should begin to represent the true dimensions of the oil field. When the smallest dimension of the pay zone, as measured from its center, is greater than the depth to the producing zone, the zero contour can be used to delineate the contact of the pay zone.

On the N-S contour map of the SVD values, a closed positive anomaly is centered on station 21 and coincides very well with the thickest portion of the "J" sand. The largest positive SVD value at station 21 also lies over the most rapid change in thickness of the pay zone. The average radius of this closed zero contour is 2.4 kilometers, which may be used as an estimate of the maximum depth to the disturbing body. This value is in good agreement with the actual depth to the producing layer which is 1.7 kilometers. The center of the anomaly is shifted to the north-northwest towards the source and away from the thickest portion of the pay zone by about 0.8 kilometers. Also a second positive anomaly is centered over station 26. Though this anomaly is based on only one SVD value, its location still

lies over portions of the "J" and "D" sands. Another reason for the occurrence of this second anomaly may be related to the extensive water injection program being performed on the oil field. The water injection has forced the oil to migrate from the eastern portion of the field down into the southern end. Interpreting the two zero contours as being coincident with the edge of the oil field shows good correlation between their location and the actual areal extent of the oil producing zones.

Comparison between the results of the N-S source SVD contour map with the E-W and rotated sources indicates a fair degree of similarity. The two zero contours of the N-S source still persist, but have been altered in shape and location. These variations are consistent with the theory in that the zero contours have migrated towards their respective sources and that they coincide with the edge of the oil field. These changes in the anomalies shown on the E-W and rotated source contour maps probably indicate the manner in which a specific source current couples with the producing zones.

Results from this survey are in good agreement with a similar survey performed over the Belle Creek field in Montana, reported by House (1979).

CONCLUSIONS

In review of the results reported herein, the D.C. bipole-bipole survey, performed over the Adena oil field, appeared to be able to detect a slight anomaly in apparent resistivity over the thickest portion of the "J" sand. This small anomaly was observed on only the E-W source apparent resistivity contour map. Being unconfirmed by the N-S or rotated maps, it is probably not significant.

An approximation of the second vertical derivative of the electric potential, for each source, was plotted on three contour maps which individually and as a collective whole support the premise that the areal extent and depth to the pay zone, at Adena, can be determined by the use of this non-traditional method of interpretation. The results of the Adena survey confirm results from a similar survey of the Belle Creek oil field as reported by House (1979). Based on the success met by two independent surveys performed over different oil fields, with differing geoelectric characteristics, the author concludes that the second vertical derivative technique of interpretation for D.C. bipole-bipole data is able to enhance and detect the anomaly produced by a thin oil saturated layer buried at depths equal to at least 1.7 kilometers.

It is suggested that this electrical technique be seriously considered as becoming a part of the petroleum exploration

program. Because of its inexpensive application and rapid surveying characteristics a D.C. bipole-bipole survey may someday be used to reduce the time and money expended by explorationists in the search for that increasingly elusive resource, oil.

APPENDIX IContents:

- 1) Program, New Organized Data
- 2) Program, New Matched Filter
- 3) Program, Last Match Filter
- 4) Figure 18 Original Signal After Filtering by
a 3 Point Averaging Filter.
- 5) Figure 19 Original Signal After Filtering by
a Matched Filter.
- 6) N-S and E-W Source Data Files.

In F format with the following information for each station in MKS units: (MX, MY, N1X, N1Y, N2X, N2Y, N3X, N3Y, N4X, N4Y, V1, V2, V3, V4, INS, IEW).

MX, MY - coordinates of center electrode for each station,

NXI, NYI - coordinates of the 4 bipole electrodes for each station

VI - potential differences associated with each of 4 bipoles

INS - current associated with the recording of the N-S bipoles

IEW - current associated with the recording of the E-W bipoles

```

C*****
C   PROGRAM NAME: NEW ORGANIZED DATA.
C   THIS PROGRAM IS DESIGNED TO READ EQUIVALENT VOLTAGE OFF-
C   SETS FROM TWO CHANNELS AND CONVERT THESE OFFSETS INTO
C   TRUE VOLTAGES. NEW FILES WILL THEN BE CREATED CONTAINING
C   TIMES AND THEIR ASSOCIATED TRUE VOLTAGES.
C*****
      DIMENSION ICHONE(1024),ICHTWO(1024)
      DIMENSION CHONE(2/1023),CHTWO(2/1023),T(0/960)
      DIMENSION ACHONE(2/1023),ACHTWO(2/1023)
      DO 10 I=1,1024
      READ(10,20)ICHONE(I),ICHTWO(I),IA,IB,IC
20    FORMAT(5(1X,16))
10    CONTINUE
      WRITE(4,30)
30    FORMAT(1X,'GAIN=',5)
      READ(4,40)GAIN
40    FORMAT(G)
      DO 50 J=2,1023
      ACHONE(J)=.25*ICHONE(J-1)+.50*ICHONE(J)+.25*ICHONE(J+1)
      ACHTWO(J)=.25*ICHTWO(J-1)+.50*ICHTWO(J)+.25*ICHTWO(J+1)
50    CONTINUE
      DO 60 J=2,1023
      CHONE(J)=(10.*ACHONE(J))/(16384.*GAIN)
      CHTWO(J)=(10.*ACHTWO(J))/(16384.*GAIN)
60    CONTINUE
      CHONEB=CHONE(32)
      CHONES=CHONE(32)
      CHTWOB=CHTWO(32)
      CHTWOS=CHTWO(32)
      DO 70 K=32,992
      IF(CHONE(K) .GT. CHONEB)CHONEB=CHONE(K)
      IF(CHONE(K) .LT. CHONES)CHONES=CHONE(K)
      IF(CHTWO(K) .GT. CHTWOB)CHTWOB=CHTWO(K)
      IF(CHTWO(K) .LT. CHTWOS)CHTWOS=CHTWO(K)
70    CONTINUE
      WRITE(4,80)CHONEB,CHONES,CHTWOB,CHTWOS
80    FORMAT(1X,'CHONEB= ',1X,G,'/',1X,'CHONES= ',1X,G,'/',1X,
8    'CHTWOB= ',1X,G,'/',1X,'CHTWOS= ',1X,G)
      DO 90 L=32,992
      T(L)=(L-32)*8.3333333*10.**-3.
      WRITE(1,100)T(L),CHONE(L)
      WRITE(2,100)T(L),CHTWO(L)
100   FORMAT(2G)
90    CONTINUE
      STOP
      END

```

```

C*****
C   PROGRAM NAME: NEW MATCHED FILTER.
C   THIS PROGRAM READS RAW FIELD DATA FROM FILE FOR10.DAT.
C   THE DATA CONTAINS SIGNAL AND NOISE. ONCE THE DATA IS
C   READ AND REDUCED TO TRUE VOLTAGES, THEN A MATCHED
C   FILTER IS APPLIED. THE MATCHED FILTER IS IN THE FORM
C   OF THE ORIGINAL SIGNAL, WHICH IN THIS CASE APPROXIMATES
C   A BOX CAR. THE FILTERED DATA IS THEN READ OUT INTO TWO
C   FILES:FOR01&FOR02.DAT.
C*****
      DIMENSION ICHONE(1024),ICHTWO(1024),A(60),T(0/960)
      DIMENSION CHONE(60/1020),CHTWO(60/1020),RES2(1083)
      DIMENSION ACHONE(1024),ACHTWO(1024),RES1(1083)
      DO 10 I=1,1024
      READ(10,20)ICHONE(I),ICHTWO(I)
20   FORMAT(2(1X,I6))
10   CONTINUE
      WRITE(4,30)
30   FORMAT(1X,'GAIN= ',5)
      READ(4,40)GAIN
40   FORMAT(G)
C*****
C   THE TRUE VOLTAGES ARE NOW DETERMINED BY DIVIDING OUT
C   THE GAIN AND BY MULTIPLYING BY A CONVERSION FACTOR.
C*****
      DO 50 J=1,1024
      ACHONE(J)=(10.*ICHONE(J))/(16384.*GAIN)
      ACHTWO(J)=(10.*ICHTWO(J))/(16384.*GAIN)
50   CONTINUE
C*****
C   THE DATA WILL NOW BE FILTERED BY A BOX CAR OPERATOR.
C*****
      DATA(A(I),I=12,49)/38*1.000000000/
      DATA(A(I),I=1,10)/10*-1.900000000/
      DATA(A(I),I=51,60)/10*-1.900000000/
      DATA A(11),A(50)/0.0,0.0/
      DO 60 K=1,1083
      RES1(K)=0.0
      RES2(K)=0.0
60   CONTINUE
      DO 70 N=1,60
      DO 70 M=1,1024
      L=M+N-1
      RES1(L)=ACHONE(M)*A(N)+RES1(L)
      RES2(L)=ACHTWO(M)*A(N)+RES2(L)
70   CONTINUE
      DO 80 I=60,1020
      CHONE(I)=RES1(I)/38.0
      CHTWO(I)=RES2(I)/38.0
80   CONTINUE
C*****

```

```

C      THIS IS THE END OF THE FILTER.
C*****
      CHONEB=CHONE(60)
      CHONES=CHONE(60)
      CHTWOB=CHTWO(60)
      CHTWOS=CHTWO(60)
      DO 90 K=60,1020
      IF(CHONE(K) .GT. CHONEB)CHONEB=CHONE(K)
      IF(CHONE(K) .LT. CHONES)CHONES=CHONE(K)
      IF(CHTWO(K) .GT. CHTWOB)CHTWOB=CHTWO(K)
      IF(CHTWO(K) .LT. CHTWOS)CHTWOS=CHTWO(K)
90    CONTINUE
      WRITE(4,100)CHONEB,CHONES,CHTWOB,CHTWOS
100   FORMAT(1X,'CHONEB= ',1X,G,/,1X,'CHONES= ',1X,G,/,
      81X,'CHTWOB= ',1X,G,/,1X,'CHTWOS= ',1X,G)
C*****
C      THE FILTERED DATA IS NOW WRITTEN OUT INTO TWO FILES
C      FROM WHICH THE DATA MAY BE EASILY PLOTTED.
C*****
      DO 110 L=60,1020
      T(L)=(L-60)*8.333333333*10.**-3.
      WRITE(11,120)T(L),CHONE(L)
      WRITE(12,120)T(L),CHTWO(L)
120   FORMAT(2G)
110   CONTINUE
      STOP
      END

```

```

C*****
C   PROGRAM NAME: LAST MATCH FILTER.
C   THIS PROGRAM READS RAW FIELD DATA FROM FILE FOR10.DAT.
C   THE DATA CONTAINS SIGNAL AND NOISE. ONCE THE DATA IS
C   READ AND REDUCED TO TRUE VOLTAGES, THEN A MATCHED
C   IN THE FORM OF 3 BOX CARS, WHICH IS IN THE SAME FORM
C   AS THE ORIGINAL SIGNAL, IS CONVOLVED WITH THE SIGNAL.
C   THE FILTERED DATA AND ASSOCIATED TIME IS READ INTO
C   FILES:FOR01&FOR02.DAT.
C*****
      DIMENSION ICHONE(1024),ICHTWO(1024),A(180),T(0/840)
      DIMENSION CHONE(180/1020),CHTWO(180/1020),RES2(1203)
      DIMENSION ACHONE(1024),ACHTWO(1024),RES1(1203)
      DO 10 I=1,1024
      READ(10,20)ICHONE(I),ICHTWO(I)
20   FORMAT(2(1X,I6))
10   CONTINUE
      WRITE(4,30)
30   FORMAT(1X,'GAIN= ',S)
      READ(4,40)GAIN
40   FORMAT(G)
C*****
C   THE TRUE VOLTAGES ARE NOW DETERMINED BY DIVIDING OUT
C   THE GAIN AND BY MULTIPLYING BY A CONVERSION FACTOR.
C*****
      DO 50 J=1,1024
      ACHONE(J)=(10.*ICHONE(J))/(15384.*GAIN)
      ACHTWO(J)=(10.*ICHTWO(J))/(15384.*GAIN)
50   CONTINUE
C*****
C   THE DATA WILL NOW BE FILTERED BY A BOX CAR OPERATOR.
C*****
      DATA(A(I),I=12,49)/38*1.000000000/
      DATA(A(I),I=1,10)/10*-1.900000000/
      DATA(A(I),I=51,60)/10*-1.900000000/
      DATA A(11),A(50)/0.0,0.0/
      DO 54 I=61,120
      A(I)=A(I-60)
54   CONTINUE
      DO 56 I=121,180
      A(I)=A(I-120)
56   CONTINUE
      DO 60 K=1,1203
      RES1(K)=0.0
      RES2(K)=0.0
60   CONTINUE
      DO 70 N=1,180
      DO 70 M=1,1024
      L=M+N-1
      RES1(L)=ACHONE(M)*A(N)+RES1(L)
      RES2(L)=ACHTWO(M)*A(N)+RES2(L)

```

```

70   CONTINUE
      DO 80 I=180,1020
          CHONE(I)=RES1(I)/114.0
          CHTWO(I)=RES2(I)/114.0
80   CONTINUE
C*****
C   THIS IS THE END OF THE FILTER.
C*****
      CHONEB=CHONE(180)
      CHONES=CHONE(180)
      CHTWOB=CHTWO(180)
      CHTWOS=CHTWO(180)
      DO 90 K=180,1020
          IF(CHONE(K) .GT. CHONEB)CHONEB=CHONE(K)
          IF(CHONE(K) .LT. CHONES)CHONES=CHONE(K)
          IF(CHTWO(K) .GT. CHTWOB)CHTWOB=CHTWO(K)
          IF(CHTWO(K) .LT. CHTWOS)CHTWOS=CHTWO(K)
90   CONTINUE
      WRITE(4,100)CHONEB,CHONES,CHTWOB,CHTWOS
100  FORMAT(1X,'CHONEB= ',1X,G,/,1X,'CHONES= ',1X,G,/,
          81X,'CHTWOB= ',1X,G,/,1X,'CHTWOS= ',1X,G)
C*****
C   THE FILTERED DATA IS NOW WRITTEN OUT INTO TWO FILES
C   FROM WHICH THE DATA MAY BE EASILY PLOTTED.
C*****
      DO 110 L=180,1020
          T(L)=(L-180)*8.333333333*10.**-3.
          WRITE(20,120)T(L),CHONE(L)
          WRITE(21,120)T(L),CHTWO(L)
120  FORMAT(2G)
110  CONTINUE
      STOP
      END

```

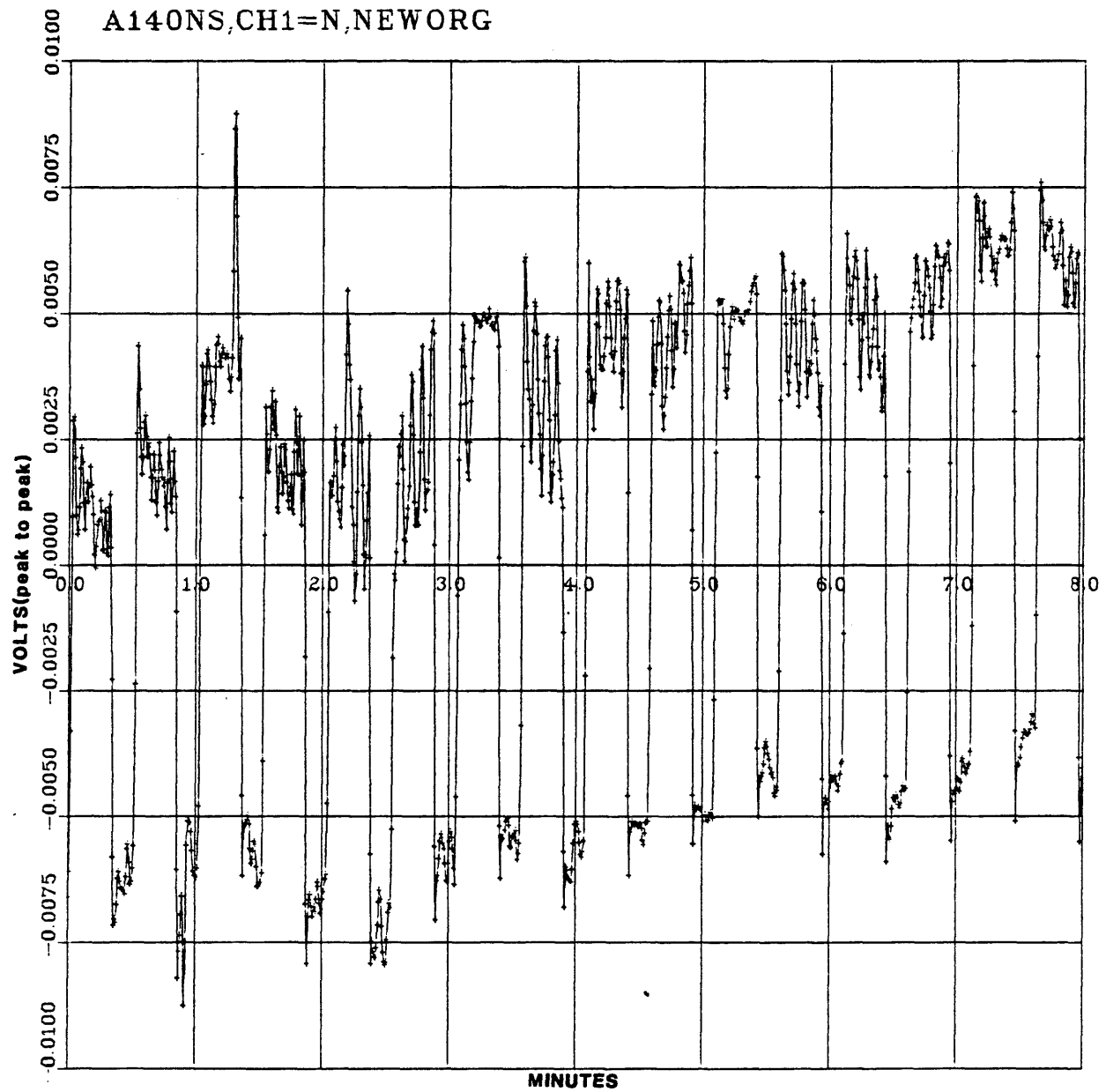


FIGURE 18 Original signal after filtering by a 3 point averaging filter.
Station 40, north bipole receiver, N-S source.

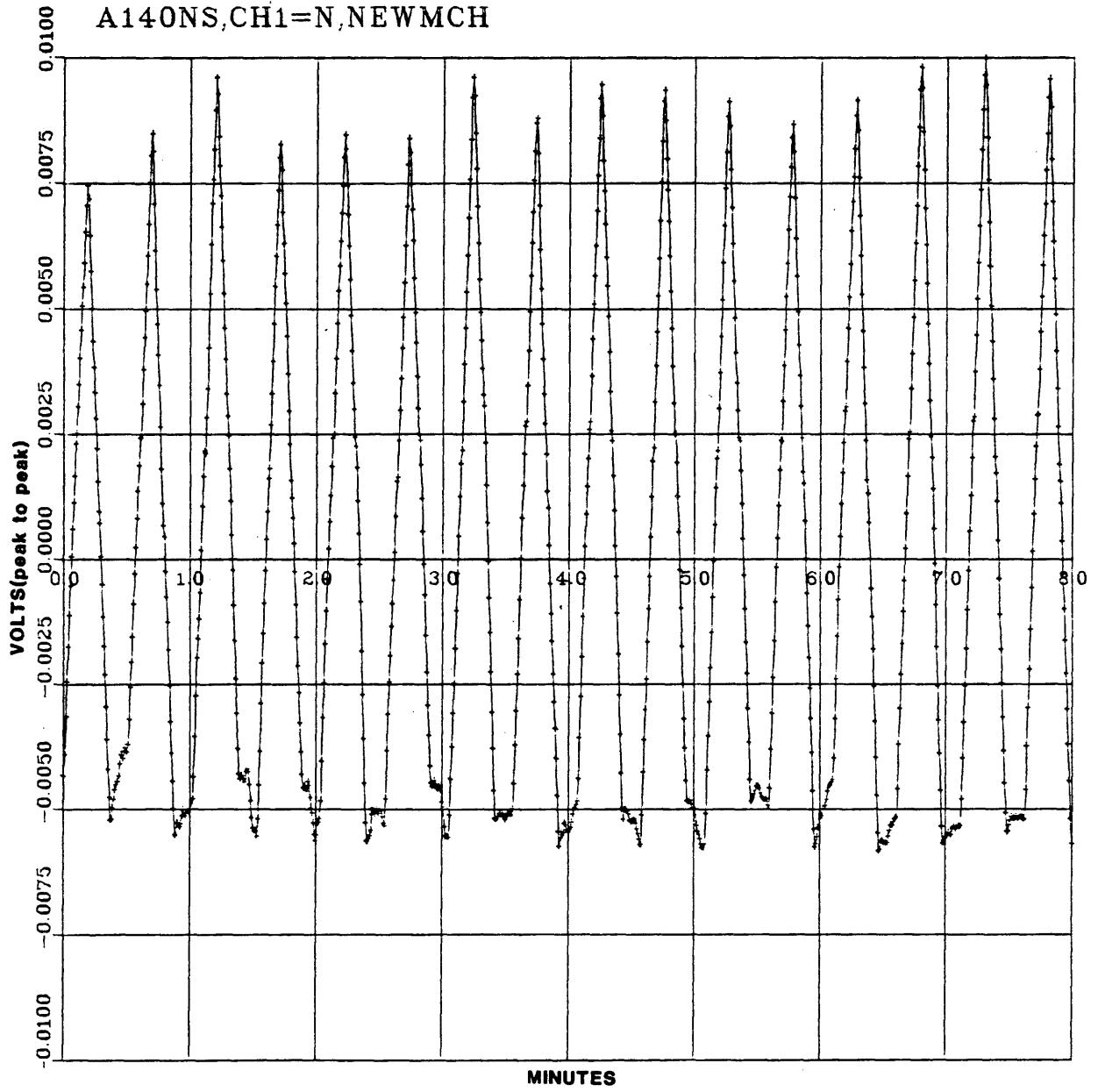


FIGURE 19 Original signal after filtering by a matched filter.

Station 40, north bipole receiver, N-S source.

N-S SOURCE DATA FILE

STATION
6-7988, 8,-1929, 4, 7988, 8,-1130, 8, 7985, 8,-2734, 1, 8793, 5,-1932, 4, 7193, 3,-1923, 3,-0.0003894, 0.0003432, -, 0.001992, 0.0002465, 149.8, 149.5
14-6379, 5,-1938, 5, 6382, 5,-1146, 0, 6376, 4,-2743, 2, 7184, 1,-1938, 5, 5580, 9,-1938, 5,-0.0005665, 0.0004754, -, 0.0003383, 0.0004776, 144.2, 144.0
16-6394, 7,-350, 5, 6388, 6, 454, 2, 6379, 5,-1146, 0, 7196, 3,-350, 5, 5593, 1,-356, 6,-0.0007547, 0.0006847, -, 0.0001512, 0.001930, 142.8, 142.2
20-4777, 6, 2859, 0, 4806, 7, 3657, 6, 4797, 6, 2054, 4, 5602, 2, 2840, 7, 3999, 0, 2852, 9, 0.0000000, 0.0000000, -, 0.0007031, 0.000828, 147.5, 146.0
21-4791, 5, 1255, 8, 4794, 5, 2048, 3, 4788, 4, 451, 1, 5593, 1, 1258, 8, 3992, 9, 1258, 8,-0.002980, 0.006750, -, 0.0005681, 0.0007363, 146.0, 144.2
22-4791, 5,-350, 5, 4791, 5, 454, 2, 4788, 4,-1152, 1, 5590, 0,-347, 5, 3989, 8,-341, 4,-0.0005670, 0.004880, -, 0.0003280, 0.0009205, 171.5, 177.0
23-4779, 3,-1938, 5, 4782, 3,-1143, 0, 4776, 2,-2740, 2, 5577, 8,-1938, 5, 3977, 6,-1935, 5,-0.0003020, 0.0002560, -, 0.0007313, 0.0010606, 150.0, 152.0
24-4776, 2,-3541, 8, 4779, 3,-2743, 2, 4779, 3,-4340, 4, 5574, 8,-3526, 5, 3974, 6,-3535, 7, 0.0000000, 0.0000000, -, 0.0001068, 0.0001068, 151.0, 152.0
26-4767, 1,-6748, 3, 4770, 1,-5943, 6, 4761, 0,-7549, 9, 5568, 7,-6742, 2, 3965, 4,-6745, 2, 0.0009325, -, 0.000171, -, 0.0003153, 0.0003172, 152.0, 148.0
33-3185, 2,-329, 2, 3182, 1, 472, 4, 3182, 1,-1133, 9, 3989, 8,-341, 4, 2389, 6,-323, 1,-0.003243, 0.012051, 0.001504, 0.001225, 148.8, 146.0
36-5200, 4, 4471, 4, 3206, 5, 5273, 0, 3194, 3, 3566, 7, 3999, 0, 4468, 4, 2407, 9, 4477, 5, 0.002446, -, 0.003554, 0.004754, -, 0.0006396, 0.0006396, 152.3, 153.3
40-1594, 1,-310, 9, 1600, 2, 493, 8, 1603, 2,-1112, 5, 2392, 7,-323, 1, 798, 6,-306, 3,-0.009016, -, 0.0157, -, 0.005149, 0.07348, 162.0, 162.0
41-1591, 1,-1911, 1, 1594, 1,-1112, 5, 1591, 1,-2712, 7, 2380, 5, 1920, 2, 792, 5,-1902, 0, 0.004482, -, 0.0031, -, 0.0047813, 0.0048038, 152.0, 152.0
48-9604, 2,-320, 0, 9607, 3, 478, 5, 9601, 2,-1118, 6, 10405, 9,-323, 1, 8802, 6,-326, 1,-0.0003480, 0.0003314, -, 0.0007664, 0.0001230, 151.5, 150.4

E-W SOURCE DATA FILE

STATION
6-7988, 8,-1929, 4, 7988, 8,-1130, 8, 7985, 8,-2734, 1, 8793, 5,-1932, 4, 7193, 3,-1923, 3, 0.0004239, -, 0.0005384, -, 0.0005374, 0.0005846, 306.5, 306.0
14-6379, 5,-1938, 5, 6382, 5,-1146, 0, 6376, 4,-2743, 2, 7184, 1,-1938, 5, 5580, 9,-1938, 5, 0.0009022, -, 0.0010956, -, 0.000894, 0.001388, 365.0, 370.0
16-6394, 7,-350, 5, 6388, 6, 454, 2, 6379, 5,-1146, 0, 7196, 3,-350, 5, 5593, 1,-356, 6, 0.0003236, -, 0.0006204, -, 0.0009556, 0.001313, 300.0, 300.0
20-4777, 6, 2859, 0, 4806, 7, 3657, 6, 4797, 6, 2054, 4, 5602, 2, 2840, 7, 3999, 0, 2852, 9, -, 0.0007010, 0.0006770, -, 0.0010800, 0.0011750, 302.5, 305.0
21-4791, 5, 1255, 8, 4794, 5, 2048, 3, 4788, 4, 451, 1, 5593, 1, 1258, 8, 3992, 9, 1258, 8,-0.004526, 0.0003008, -, 0.0016875, 0.0026519, 305.0, 301.9
22-4791, 5,-350, 5, 4791, 5, 454, 2, 4788, 4,-1152, 1, 5590, 0,-347, 5, 3989, 8,-341, 4, 0.0002240, -, 0.0003124, -, 0.001717, 0.003020, 304.4, 300.0
23-4779, 3,-1938, 5, 4782, 3,-1143, 0, 4776, 2,-2740, 2, 5577, 8,-1938, 5, 3977, 6,-1935, 5, 0.0004888, -, 0.0006831, -, 0.0011731, 0.0015750, 307.5, 305.0
24-4776, 2,-3541, 8, 4779, 3,-2743, 2, 4779, 3,-4340, 4, 5574, 8,-3526, 5, 3974, 6,-3535, 7, 0.0004408, -, 0.001108, -, 0.0005099, 0.0002569, 305.0, 307.0
26-4767, 1,-6748, 3, 4770, 1,-5943, 6, 4761, 0,-7549, 9, 5568, 7,-6742, 2, 3965, 4,-6745, 2, 0.0009881, -, 0.0007747, 0.0004276, -, 0.0005926, 0.0005926, 306.9, 302.5
28-4779, 3,-5138, 9, 4779, 3,-4346, 4, 4773, 1,-5940, 5, 5577, 8,-5120, 6, 3977, 6,-5132, 8,-0.001305, 0.001293, 0.0000000, 0.0000000, 305.0, 340.0
33-3185, 2,-329, 2, 3182, 1, 472, 4, 3182, 1,-1133, 9, 3989, 8,-341, 4, 2389, 6,-323, 1,-0.00252, -, 0.0026273, -, 0.00252, -, 0.003625, 0.003625, 340.0, 340.0
40-1594, 1,-310, 9, 1600, 2, 493, 8, 1603, 2,-1112, 5, 2392, 7,-323, 1, 798, 6,-306, 3,-0.001195, -, 0.002221, -, 0.002534, 0.00300, 304.4
41-1591, 1,-1911, 1, 1594, 1,-1112, 5, 1591, 1,-2712, 7, 2380, 5, 1920, 2, 792, 5,-1902, 0, 0.0078627, -, 0.0045038, -, 0.0041873, 0.0036413, 305.0, 308.0
48-9604, 2,-320, 0, 9607, 3, 478, 5, 9601, 2,-1118, 6, 10405, 9,-323, 1, 8802, 6,-326, 1, 0.0005952, -, 0.0002255, -, 0.0004363, 0.0005971, 306.0, 305.0
47-9598, 2,-1926, 3, 9589, 0,-1124, 7, 9595, 1,-2721, 9, 10399, 8,-1932, 4, 8799, 6,-1932, 4, 0.0003221, -, 0.0003626, -, 0.0003141, 0.0003839, 303.0, 302.5

APPENDIX 2

Contents:

- 1) Program, Apparent Resistivity
- 2) Program, Total Field Apparent Resistivity

```

C*****
C   PROGRAM NAME: APPARENT RESISTIVITY.
C   THIS PROGRAM WILL CALCULATE THE APPARENT RESISTIVITY
C   OF THE EARTH RESULTING FROM A BIPOLE SOURCE OF CURRENT
C   BEING MEASURED BY A BIPOLE RECEIVER. THE CURRENT
C   ELECTRODES +A AND -B IMPRESS A CURRENT I INTO THE
C   GROUND AND THE RECEIVER ELECTRODES M AND NI MEASURE
C   THE CHANGE IN THE ELECTRIC POTENTIAL U. PARAMETERS:
C   N=THE NUMBER OF NI ELECTRODES, +A AT (AX,AY),-B AT (0,0).
C*****
      IMPLICIT REAL (M)
      IMPLICIT REAL (N)
      DIMENSION MX(11),MY(11),NX(44),NY(44),AMP(44)
      DIMENSION UMN(44),AM(44),BM(44),AN(44),BN(44)
      DIMENSION APPRES(44),D(44)
      WRITE(4,10)
10     FORMAT(1X,'N= ',5)
      READ(4,20)N
20     FORMAT(G)
      WRITE(4,30)
30     FORMAT(1X,'AX= ',5)
      READ(4,20)AX
      WRITE(4,40)
40     FORMAT(1X,'AY= ',5)
      READ(4,20)AY
C*****
C   THE LOCATION FOR ALL M RECEIVER ELECTRODES IS ENTERED.
C*****
      DATA(MX(I),I=1,4)/3185.2,1594.1,1591.1,7988.8/
      DATA(MY(I),I=1,4)/-329.2,-310.9,-1911.1,-1929.4/
      DATA(MX(I),I=5,8)/6379.5,6394.7,4791.5,4791.5/
      DATA(MY(I),I=5,8)/-1938.5,-350.5,1255.8,-350.5/
      DATA(MX(I),I=9,11)/4779.3,4767.1,9604.2/
      DATA(MY(I),I=9,11)/-1938.5,-6748.3,-320.0/
      DATA BX,BY/0.0,0.0/
C*****
C   DATA CONTAINING THE (X,Y) LOCATION OF ALL THE NI
C   ELECTRODES AND THEIR ASSOCIATED CHANGE IN ELECTRIC
C   POTENTIALS U AND ASSOCIATED CURRENT I IS READ FROM
C   FILE FOR01.DAT.
C*****
      DO 70 I=1,N
      READ(16,80)NX(I),NY(I),UMN(I),AMP(I)
      WRITE(4,80)NX(I),NY(I),UMN(I),AMP(I)
80     FORMAT(4F)
70     CONTINUE
C*****
C   RADIAL DISTANCES ARE NOW CALCULATED.
C*****
      K=0
      DO 90 M=1,N/4

```

```

      J=1
      DO 100 I=J+K,K+4
      AM(I)=1./((MX(M)-AX)**2.+(MY(M)-AY)**2.)**.5
      BM(I)=1./((MX(M)-BX)**2.+(MY(M)-BY)**2.)**.5
      AN(I)=1./((NX(I)-AX)**2.+(NY(I)-AY)**2.)**.5
      BN(I)=1./((NX(I)-BX)**2.+(NY(I)-BY)**2.)**.5
100   CONTINUE
      K=K+4
90    CONTINUE
C*****
C   THE APPARENT RESISTIVITY IS NOW CALCULATED AND WILL
C   BE READ INTO FOR03.DAT.
C*****
      TWOPI=6.28318531
      DO 110 L=1,N
      D(L)=(1./(AM(L)-BM(L)-AN(L)+BN(L)))
      APPRES(L)=((TWOPI*UMN(L))/AMP(L))*D(L)
110   CONTINUE
      DO 120 K=1,N
      WRITE(3,130)NX(K),NY(K),APPRES(K)
130   FORMAT(3F)
120   CONTINUE
      STOP
      END

```

```

C*****
C   PROGRAM NAME: TOTAL FIELD APPARENT RESISTIVITY.
C   THIS PROGRAM CALCULATES THE TOTAL FIELD APPARENT RESIS-
C   TIVITY FOR THE EARTH RESULTING FROM A BIPOLE CURRENT
C   SOURCE AS MEASURED BY A DIPOLE RECEIVER. THE CURRENT
C   I IS IMPRESSED INTO THE EARTH BY BIPOLE CURRENT
C   ELECTRODES +A AND -B. THE POTENTIAL DIFFERENCE IS
C   MEASURED BY RECEIVER ELECTRODES M AND N.
C   FROM THE QUADRAPOLE RECEIVER ARRAY, 4 POSSIBLE
C   TOTAL ELECTRIC FIELD VECTORS ARE DETERMINED AND
C   THROUGH MULTIPLICATION BY A GENERALIZED GEOMETRIC
C   FACTOR, 4 APPARENT RESISTIVITIES ARE CALCULATED FOR
C   EACH OF TWO BIPOLE SOURCES. PARAMETERS: N=NUMBER
C   OF RECEIVER LOCATIONS, + POLE OF SOURCE AT (AX,AY),
C   - POLE OF SOURCE AT (BX,BY).
C*****
      IMPLICIT REAL (L)
      IMPLICIT REAL (M)
      IMPLICIT REAL (N)
      IMPLICIT REAL (I)
      DIMENSION MX(12),MY(12),N1X(12),N1Y(12),N2X(12)
      DIMENSION N2Y(12),N3X(12),N3Y(12),N4X(12),N4Y(12)
      DIMENSION V1(12),V2(12),V3(12),V4(12),INS(12)
      DIMENSION IEW(12),L1(12),L2(12),L3(12),L4(12)
      DIMENSION E1(12),E2(12),E3(12),E4(12),ET1(12)
      DIMENSION ET2(12),ET3(12),ET4(12),IAV(12),A(12)
      DIMENSION B(12),C(12),APRES1(12),APRES2(12)
      DIMENSION APRES3(12),APRES4(12)
      WRITE(4,10)
10    FORMAT(1X,'N= ',5)
      READ(4,20)N
20    FORMAT(F)
      WRITE(4,30)
30    FORMAT(1X,'AX= ',5)
      READ(4,20)AX
      WRITE(4,40)
40    FORMAT(1X,'AY= ',5)
      READ(4,20)AY
      DATA BX,BY/0.0,0.0/
C*****
C   DATA CONTAINING THE FOLLOWING PARAMETERS ARE READ FROM
C   EITHER FOR19.DAT OR FOR20.DAT. (MX,MY)-COORDINATES OF
C   THE CENTER M ELECTRODE FOR EACH SOURCE, (N1X,N1Y),I=
C   1,4 - COORDINATES OF THE 4 N ELECTRODES FOR EACH STA-
C   TION,(VI),I=1,4-POTENTIAL DIFFERENCES FOR EACH OF
C   THE 4 PAIRS OF MNI RECEIVER DIPOLES FOR EACH STATION,
C   (INS,IEW)-CURRENT ASSOCIATED WITH THE MEASUREMENT OF
C   EITHER THE NS OR EW RECEIVER PAIRS.
C*****
      DO 50 J=1,N
      READ(15,60)MX(J),MY(J),N1X(J),N1Y(J),N2X(J),N2Y(J),

```

```

        1N3X(J),N3Y(J),N4X(J),N4Y(J),V1(J),V2(J),V3(J),V4(J),
        2INS(J),IEW(J)
60   FORMAT(16F)
50   CONTINUE
C*****
C   THE 4 TOTAL ELECTRIC FIELD VECTORS ARE NOW CALCULATED
C   FOR EACH STATION.LI-LENGTH OF MNI,EI=VI/MNI,ETI-
C   THE TOTAL ELECTRIC FIELD VECTOR.
C*****
      DO 70 J=1,N
      L1(J)=((MX(J)-N1X(J))**2.+(MY(J)-N1Y(J))**2.)**.5
      L2(J)=((MX(J)-N2X(J))**2.+(MY(J)-N2Y(J))**2.)**.5
      L3(J)=((MX(J)-N3X(J))**2.+(MY(J)-N3Y(J))**2.)**.5
      L4(J)=((MX(J)-N4X(J))**2.+(MY(J)-N4Y(J))**2.)**.5
      E1(J)=V1(J)/L1(J)
      E2(J)=V2(J)/L2(J)
      E3(J)=V3(J)/L3(J)
      E4(J)=V4(J)/L4(J)
      ET1(J)=(E1(J)**2.+E3(J)**2.)**.5
      ET2(J)=(E3(J)**2.+E2(J)**2.)**.5
      ET3(J)=(E2(J)**2.+E4(J)**2.)**.5
      ET4(J)=(E4(J)**2.+E1(J)**2.)**.5
70   CONTINUE
C*****
C   DISTANCES FROM SOURCE ELECTRODES TO THE CENTER OF EACH
C   STATION ARE NOW CALCULATED.YA=Y DISTANCE BETWEEN +A
C   AND M ELECTRODE,YB=SAME FOR -B AND M.XA=X DISTANCE
C   BETWEEN +A AND M ELECTRODE,XB=SAME FOR -B AND M.
C   AM=RADIAL DISTANCE BETWEEN +A AND M,BM=SAME FOR -B AND M.
C   IAV=THE AVERAGE OF THE CURRENTS IMPRESSED DURINGTHE
C   THE MEASUREMENT OF POTENTIAL FOR NS AND EW RECEIVERS.
C*****
      DO 80 J=1,N
      XA(J)=MX(J)-AX
      YA(J)=MY(J)-AY
      XB(J)=MX(J)-BX
      YB(J)=MY(J)-BY
      AM(J)=((MX(J)-AX)**2.+(MY(J)-AY)**2.)**.5
      BM(J)=((MX(J)-BX)**2.+(MY(J)-BY)**2.)**.5
      A(J)=((YA(J)/AM(J)**3.)-(YB(J)/BM(J)**3.))**2.
      B(J)=((XA(J)/AM(J)**3.)-(XB(J)/BM(J)**3.))**2.
      C(J)=1./((A(J)+B(J))**.5)
      IAV(J)=(INS(J)+IEW(J))/2.
80   CONTINUE
C*****
C   THE TOTAL FIELD APPARENT RESISTIVITY IS NOW CALCULATED
C   FOR EACH STATION. FOR EACH STATION THERE WILL BE 4
C   POSSIBLE TOTAL FIELD APPARENT RESISTIVITIES GENERATED
C   FROM THE TOTAL FIELD VECTORS ET1,ET2,ET3 AND ET4.
C*****
      TWOPI=6.28318531

```

```
      DO 90 J=1,N
      APRES1(J)=((ET1(J)*TWOPI)/IAV(J))*C(J)
      APRES2(J)=((ET2(J)*TWOPI)/IAV(J))*C(J)
      APRES3(J)=((ET3(J)*TWOPI)/IAV(J))*C(J)
      APRES4(J)=((ET4(J)*TWOPI)/IAV(J))*C(J)
90    CONTINUE
C*****
C THE 4 APPARENT RESISTIVITIES AND THEIR ASSOCIATED STA-
C TION CENTER M ELECTRODES ARE NOW WRITTEN INTO
C FOR21.DAT.
C*****
      DO 100 J=1,N
      WRITE(21,110)MX(J),MY(J),APRES1(J),APRES2(J),
1    APRES3(J),APRES4(J)
110  FORMAT(6F)
100  CONTINUE
      STOP
      END
```

APPENDIX 3

Contents:

- 1) Program, Second Vertical Derivative of a Uniform
Earth

```

C*****
C   PROGRAM NAME: SECOND VERTICAL DERIVATIVE OF A
C                   UNIFORM EARTH.
C   THIS PROGRAM CALCULATES THE SECOND VERTICAL DERIVATIVE
C   (SVD) OF THE ELECTRIC POTENTIAL FOR A UNIFORM HALF-SPACE
C   RESULTING FROM A DIPOLE CURRENT IMPRESSED ON THE Z=0
C   SURFACE. PARAMETERS:RHO=1.0 OHMM,N=NUMBER OF POINTS ON
C   Z=0, FOR WHICH THE SVD IS TO BE DETERMINED,(XL,YL)=THE
C   COORDINATES OF THE + POLE OF THE DIPOLE, - AT (0,0).
C*****
      DIMENSION XN(15),YN(15),IN(15),A(15),B(15),C(15)
      DIMENSION D(15),E(15),F(15),SVDU(15)
      WRITE(4,10)
10     FORMAT(1X,'N= ',5)
      READ(4,20)N
20     FORMAT(G)
      WRITE(4,30)
30     FORMAT(1X,'XL= ',5)
      READ(4,20)XL
      WRITE(4,40)
40     FORMAT(1X,'YL= ',5)
      READ(4,20)YL
      DATA RHO,TWOPI/1.0000000,6.28318531/
C*****
C   THE DATA WILL NOW BE READ FROM FOR10.DAT. THE VARIABLES
C   ARE (XN,YN)=COORDINATES OF THE POINT AT WHICH THE SVD
C   IS TO BE DETERMINED,IN=THE CURRENT ASSOCIATED AT THE POINT.
C*****
      DO 50 I=1,N
      READ(13,60)XN(I),YN(I),IN(I)
60     FORMAT(3G)
50     CONTINUE
C*****
C   THE SVD IS NOW CALCULATED FOR EACH POINT.
C*****
      DO 70 I=1,N
      A(I)=(XN(I)-XL)**2.
      B(I)=(YN(I)-YL)**2.
      C(I)=XN(I)**2.
      D(I)=YN(I)**2.
      E(I)=- (A(I)+B(I))**-.5
      F(I)=(C(I)+D(I))**-.5
      SVDU(I)=((RHO*IN(I))/(TWOPI))*(E(I)+F(I))
70     CONTINUE
C*****
C   THE SVD AND ITS ASSOCIATED COORDINATES WILL BE WRITTEN
C   INTO FOR12.DAT.
C*****
      DO 90 I=1,N
      WRITE(12,90)XN(I),YN(I),SVDU(I)
90     FORMAT(3G)

```

30 CONTINUE
 STOP
 END

APPENDIX 4Contents:

Examples of Filtered Data:

- 1) Using a 3 Point Averaging Filter.
- 2) Using a Matched Filter in the Form of a Square Wave.
- 3) Using a Matched Filter in the Form of 3 Square Waves.

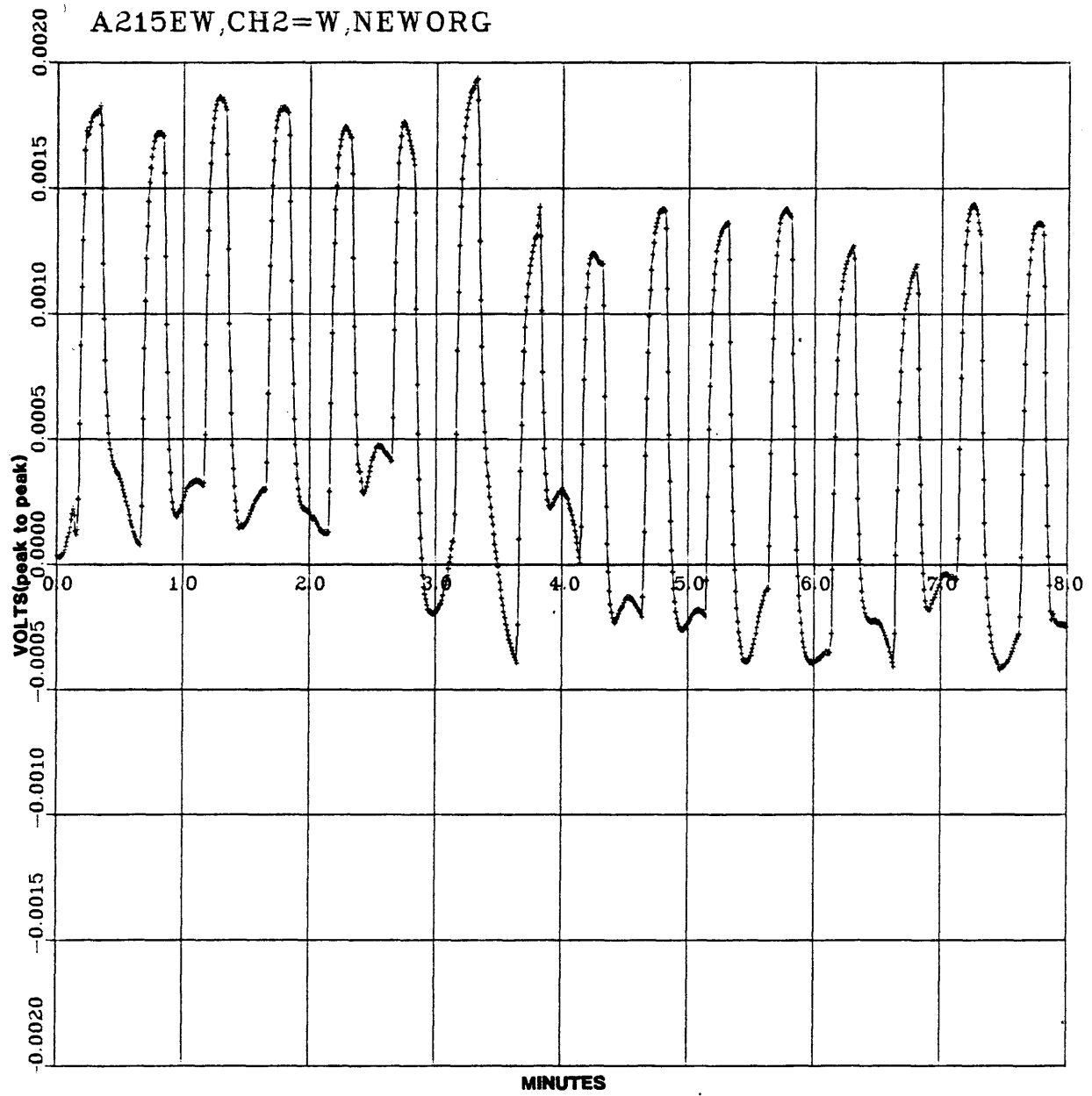


FIGURE 20 Original signal after filtering by a 3 point averaging filter.

Station 15, west bipole receiver, E-W source.

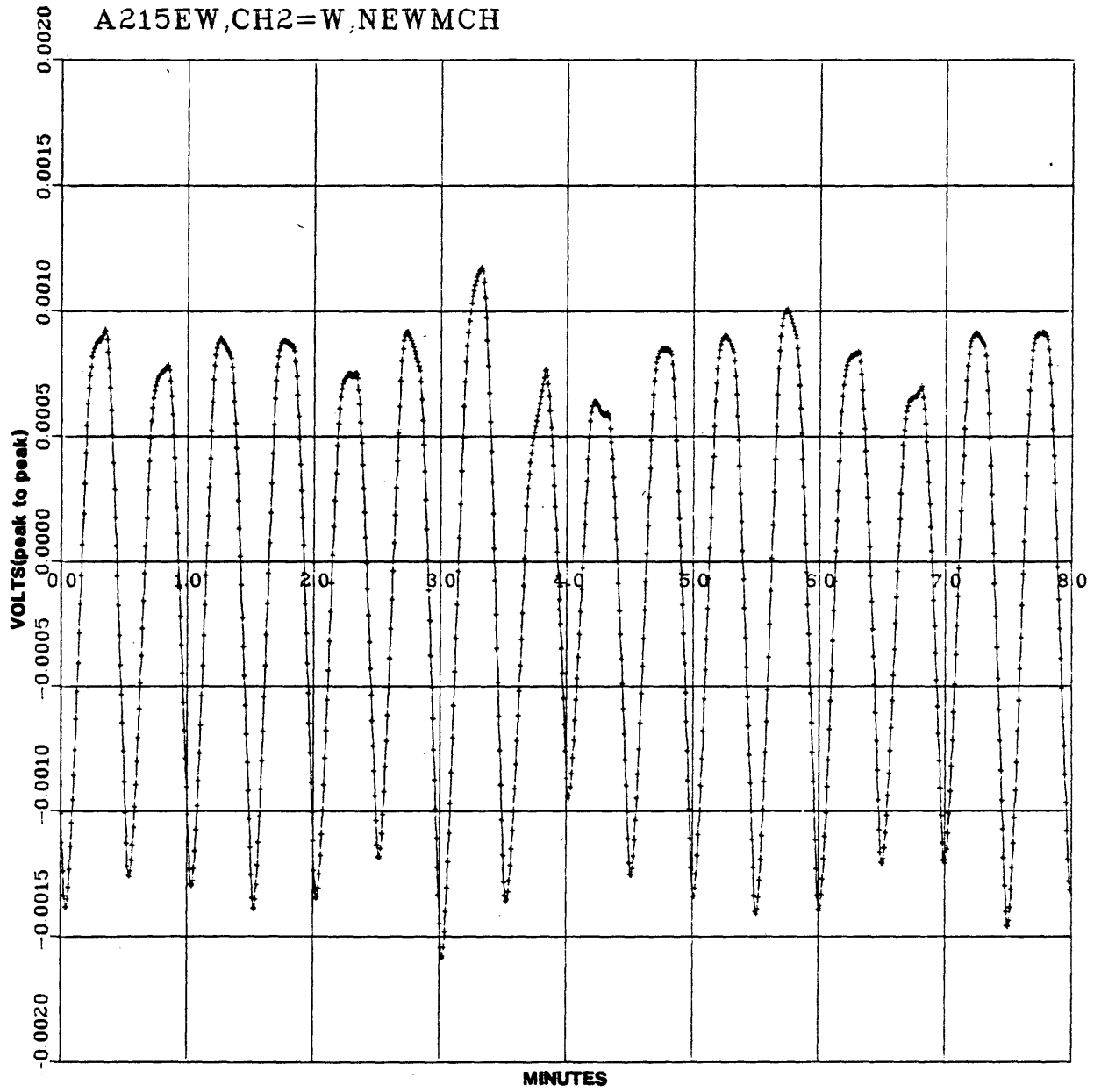


FIGURE 21 Original signal after filtering by a matched filter.

Station 15, west bipole receiver, E-W source.

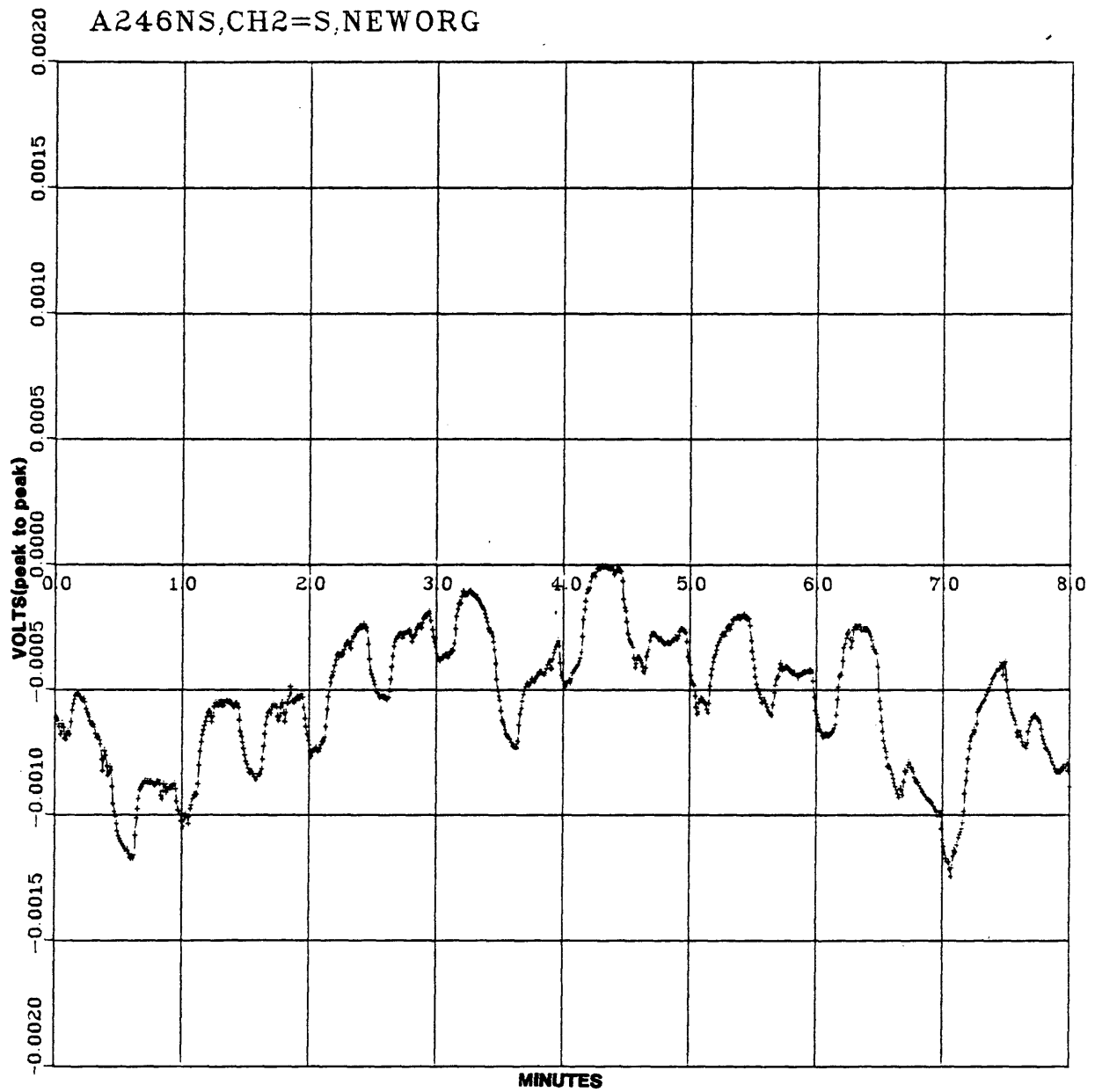


FIGURE 22 Original signal after filtering by a 3 point averaging filter.
Station 46, south bipole receiver, E-W source.

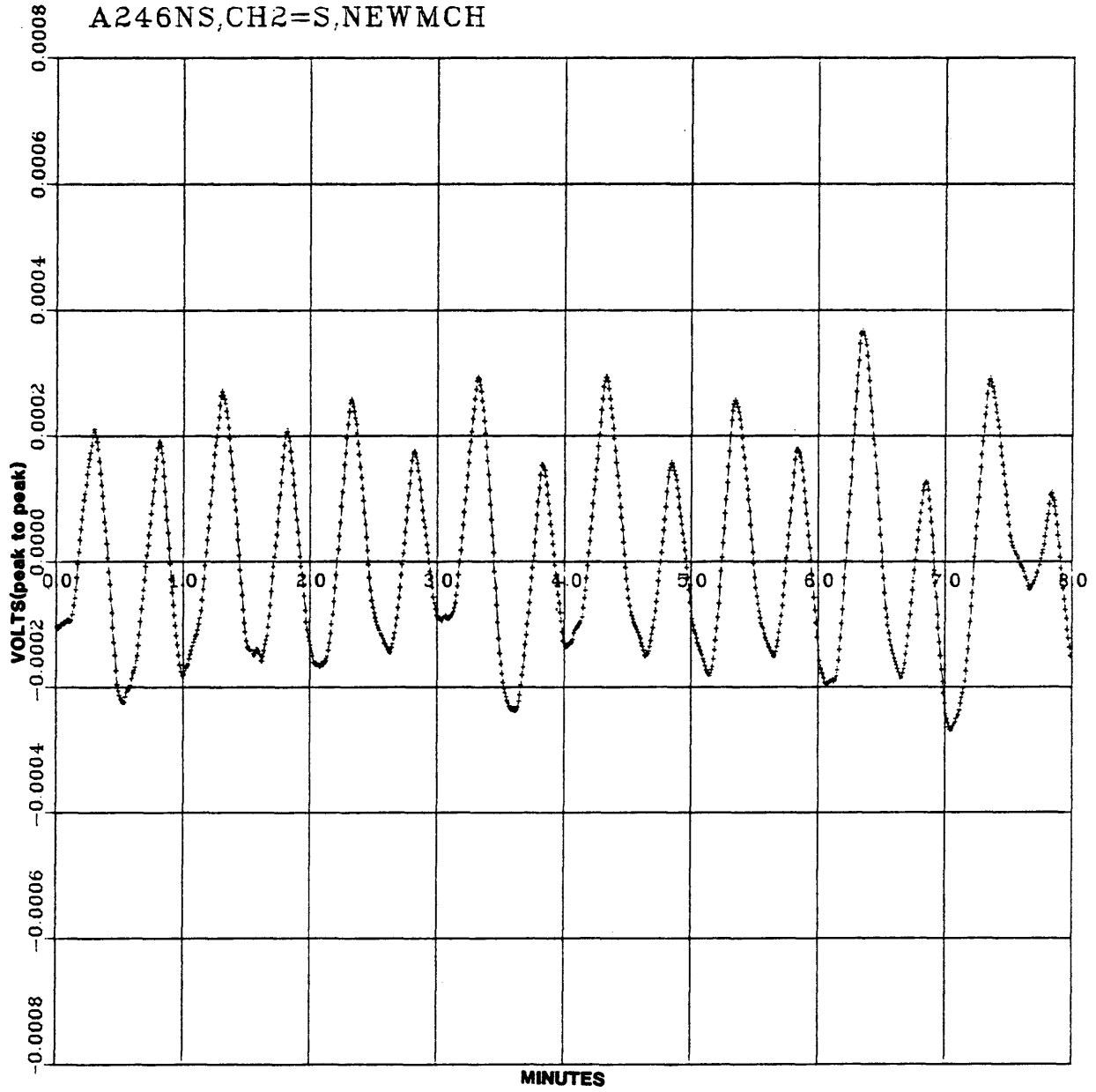


FIGURE 23 Original signal after filtering by a matched filter.
Station 46, south bipole receiver, E-W source.

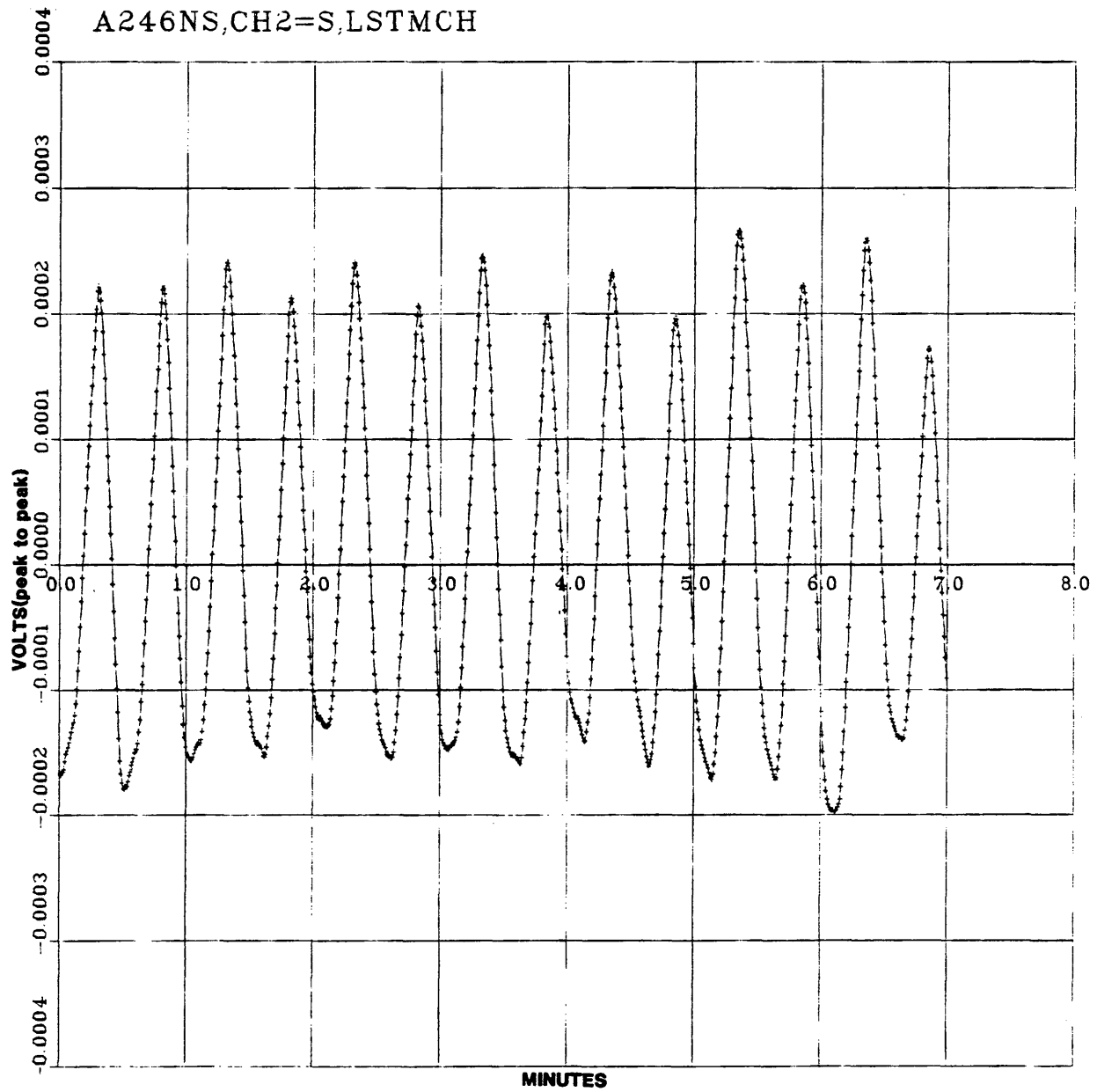


FIGURE 24 Original signal after filtering by the matched filter Last Match.
Station 46, south bipole receiver, E-W source.

BIBLIOGRAPHY

- Alpin, L.M., 1966, The Theory of Dipole Soundings, New York, Consultants Bureau Enterprises, Dipole Methods For Measuring Earth Conductivity, pp. 1-60.
- Cullen, A.W., Forcade, K.C., 1954, Geology of the Adena Field, Denver, Rocky Mountain Association of Geologists, The Oil and Gas Fields of Colorado, pp. 77-78.
- Evjen, H.M., 1936, The Place of the Vertical Gradient in Gravitational Interpretations, Geophysics, Vol. 1, No. 1, pp. 127-136.
- Henderson, R.G., Zietz, I., Graphical Calculation of Total-Intensity Anomalies of Three-Dimensional Bodies, Geophysics, Vol. 22, No. 4, pp. 887-904.
- House, N.J., 1979, Modified Bipole-Dipole Survey Belle Creek Oil Field, Colorado School of Mines, Masters Thesis, T-2203, unpublished.
- Kaufman, A.A., 1980, Personal communications.
- Keller, G.V., Frischnecht, F.C., 1966, Electrical Methods in Geophysical Prospecting, Oxford, Pergamon Press, Inc.
- Keller, G.V., 1968, Electrical Prospecting for Oil, Golden, C.S.M. Publications, C.S.M. Quarterly, Vol. 63, No. 2.
- Keller, G.V., 1969, Electro-Magnetic Surveys in the Central Volcanic Region, Preliminary Report, New Zealand, Department of Scientific and Industrial Research of N.Z., Report 55, unpublished.
- Keller, G.V., 1980, Personal communications.
- Keller, G.V., 1979, Research on Direct Detection of Oil and Gas Reservoirs Using Electrical Methods, Golden, C.S.M. Geophysics Department, Annual Technical Report, I.G.P., 1978-1979, unpublished, pp. 11-15.
- Keller, G.V., Furgerson, R.B., Harthill, N., Jacobson, J.J., 1975, The Dipole Mapping Method, Geophysics, Vol. 40, No. 3, pp. 451-472.
- Keller, G.V., Theory of Quasi-Direct Location of Oil with Electrical Prospecting Methods, unpublished.

- Meinardus, H.A., 1967, A Model Study of Kernel Functions for the Adena Oil Field, Morgan County, Colorado, Colorado School of Mines, Doctorial Thesis, T-1103, unpublished.
- Murry, H.F., 1957, Stratigraphic Traps in Denver Basin, Bulletin of the American Association of Petroleum Geologists, Vol. 41, No. 5, pp. 839-847.
- Mygdal, K.A., 1963, Adena-Largest Field in Denver Basin, Denver, R.M.A.G., Geology of the Northern Denver Basin and Adjacent Uplifts, pp. 222-225.
- Perry, L.M., Overstake, H.D.; 1955, The Adena Field, The Pure Oil Company, Denver District, unpublished.
- Peters, L.J., 1949, The Direct Approach to Magnetic Interpretation and Its Practical Application, Geophysics, Vol. 14, No. 3, pp. 290-320.
- Stoyer, C.H., 1980, Personal communications.
- Tietz, F.A., 1956, The Adena Oil Field Area, Morgan and Adams Counties, Colorado, University of Colorado at Boulder, Masters Thesis, unpublished.
- Valla, P., 1979, An Electromagnetic Sounding Survey by the D.C. Null-Point Method in the Northern San Luis Valley, unpublished.
- Van Nostrand, R.G., Cook, K.L., 1966, Interpretation of Resistivity Data, Washington, U.S.G. Printing Office, G.S. Professional Paper 499.
- Whan, W.J., 1979, Numerical Modeling of the Direct Current Resistivity for Thin Insulators, Colorado School of Mines, Doctorial Thesis, T-2231, unpublished.
- Zohdy, A.A.R., 1978, Total Field Resistivity Mapping and Sounding Over Horizontally Layered Media, Geophysics, Vol. 43, No. 4, pp. 748-766.